Stem Cell Reports
Resource
OPEN ACCESS

Defined Conditions for the Isolation and Expansion of Basal Prostate Progenitor Cells of Mouse and Human Origin

Thomas Höfner,[1] Christian Eisen,[1] Corinna Klein,[1] Teresa Rigo-Watermeier,[2] Stephan M. Goeppinger,[4] Anna Jauch,[5] Brigitte Schoell,[5] Vanessa Vogel,[1] Elisa Noll,[1] Wilko Weichert,[4] Irène Baccelli,[1] Anja Schillert,[2] Steve Wagner,[2] Sascha Pahernik,[3] Martin R. Sprick,[1,7,*] and Andreas Trumpp[1,2,6,7,*]
[1]Heidelberg Institute for Stem Cell Technology and Experimental Medicine (HI-STEM gGmbH), 69120 Heidelberg, Germany
[2]Division of Stem Cells and Cancer, Deutsches Krebsforschungszentrum (DKFZ), 69120 Heidelberg, Germany
[3]Department of Urology, University Hospital Heidelberg, 69120 Heidelberg, Germany
[4]Institute of Pathology, University Hospital Heidelberg, 69120 Heidelberg, Germany
[5]Department of Human Genetics, University Hospital Heidelberg, 69120 Heidelberg, Germany
[6]German Cancer Consortium (DKTK), 69120 Heidelberg, Germany
[7]Co-senior author
*Correspondence: martin.sprick@hi-stem.de (M.R.S.), a.trumpp@dkfz.de (A.T.)
http://dx.doi.org/10.1016/j.stemcr.2015.01.015

SUMMARY

Methods to isolate and culture primary prostate epithelial stem/progenitor cells (PESCs) have proven difficult and ineffective. Here, we present a method to grow and expand both murine and human basal PESCs long term in serum- and feeder-free conditions. The method enriches for adherent mouse basal PESCs with a $Lin^{-}SCA\text{-}1^{+}CD49f^{+}TROP2^{high}$ phenotype. Progesterone and sodium selenite are additionally required for the growth of human $Lin^{-}CD49f^{+}TROP2^{high}$ PESCs. The gene-expression profiles of expanded basal PESCs show similarities to ESCs, and NF-kB function is critical for epithelial differentiation of sphere-cultured PESCs. When transplanted in combination with urogenital sinus mesenchyme, expanded mouse and human PESCs generate ectopic prostatic tubules, demonstrating their stem cell activity in vivo. This novel method will facilitate the molecular, genomic, and functional characterization of normal and pathologic prostate glands of mouse and human origin.

INTRODUCTION

Several model systems have been developed to understand the pathologically altered pathways observed during benign prostatic enlargement and prostate cancer, the latter being the most common type of cancer in men. It has been suggested that epithelial stem/progenitor cells (PESCs) are critical for the regulation and maintenance of the prostatic gland and that they also play an important role in prostate cancer development (Choi et al., 2012; Goldstein et al., 2010; Lu et al., 2013; Visvader, 2011; Wang et al., 2009). PESCs, like other somatic tissue stem cells, are thought to be rare, with a frequency of 1%–5% (Goldstein et al., 2011; Lukacs et al., 2010). Isolation and ex vivo expansion of PESCs is further complicated by their dependence on poorly understood factors supplied by a prostate stem cell niche composed of smooth muscle cells, fibroblasts, neuroendocrine cells, and differentiating and mature prostate epithelial cells (Goldstein et al., 2010; Morrison and Spradling, 2008; Wang et al., 2009). Although significant progress has been made, current culture techniques allow for only limited expansion of prostate epithelial cells (PrECs), which rapidly cease to proliferate (Chaproniere and McKeehan, 1986; Litvinov et al., 2006; Rhim et al., 2011). Human telomerase reverse transcriptase (hTERT)-mediated immortalization has been used to optimize in vitro cultures of primary PrECs (Kogan et al., 2006). Although hTERT-immortalized cells have prolonged in vitro lifespans, they show significant changes compared with normal PrECs, limiting their value as a model system (Klinger et al., 2006). Culture methods using serum-free media conditions with or without additional murine 3T3 feeder cells to grow murine and human PrECs have been described, but serial passaging is limited and these strategies allow neither significant enrichment nor expansion of the stem/progenitor compartment (Kabalin et al., 1989; Peehl and Stamey, 1986; Robinson et al., 1998). In contrast, growing PrECs in semisolid medium using Matrigel facilitates their growth as prostaspheres that retain PESCs with self-renewal capacity in vitro. However, prostaspheres are difficult to manipulate, and the spheres consist of only few PESCs surrounded by a large number of more differentiated PrECs (Xin et al., 2007). More recently, dissociated murine and human PESCs were isolated by flow cytometry (fluorescence-activated cell sorting [FACS]). However, this method is limited by the low frequency of PESCs in conjunction with the small amount of material obtainable from human biopsies, as well as the lack of a suitable culture systems for maintaining or expanding undifferentiated PESCs (Goldstein et al., 2010, 2011; Lukacs et al., 2010; Miki and Rhim, 2008). Here, we report specific workflows and novel, robust,

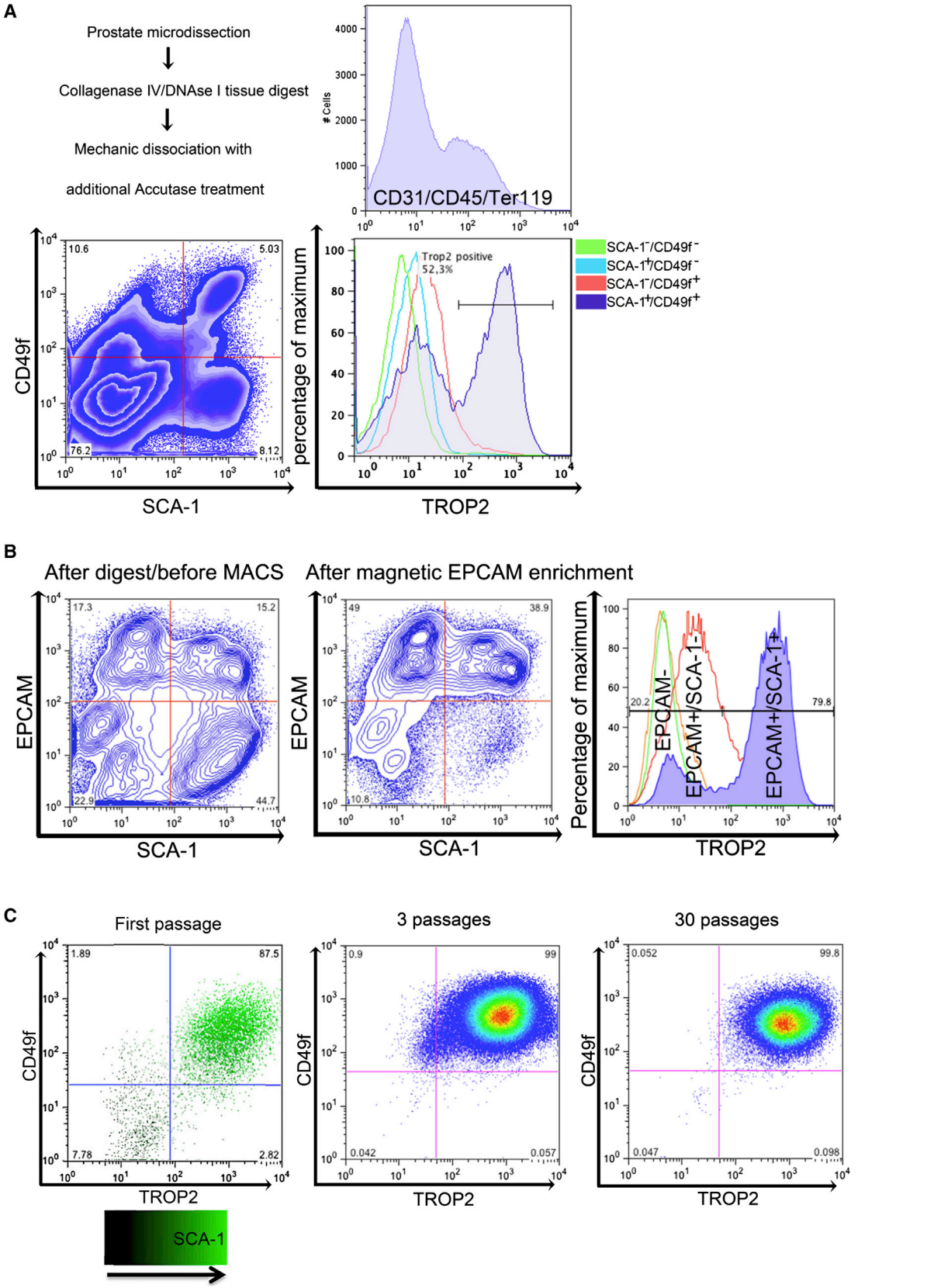

(legend on next page)

simple, serum- and feeder-free culture techniques to maintain and expand functional primary basal PESCs of mouse and human origin.

RESULTS

Expansion and Maintenance of Primary Murine Basal PESCs in Serum-free Cultures

To develop conditions that would allow us to maintain and expand ex vivo isolated primary murine PESCs, we used single-cell suspensions obtained from whole murine prostates as the starting material. FACS analysis revealed that these cell mixtures contained 4.5% ± 1.5% of SCA-1$^+$CD49f$^+$TROP2$^+$ cells, a phenotype previously used to define basal PESCs (Figures 1A and S1A; Goldstein et al., 2008, 2011; Lukacs et al., 2010). To identify which of the three markers is most critical for further enrichment of basal PESCs, we performed castration experiments. In response to castration and the associated androgen decay, a basal progenitor hyperplasia is commonly observed (Evans and Chandler, 1987; Wu et al., 2007). As expected, we found that TROP2 was robustly upregulated in the basal progenitor cells of the hyperplastic epithelium of castrated mice, confirming the previous finding that TROP2 is a specific marker for basal PESCs (Stoyanova et al., 2012). In contrast, both testosterone-treated castrated mice and unmanipulated wild-type mice displayed the presence of columnar luminal epithelial cells, with low TROP2 expression in both basal and luminal cells (Figure S1B and data not shown).

FACS analysis was used to further characterize the PrEC subpopulations. The pan-epithelial marker epithelial cell adhesion molecule (EPCAM) was expressed in both the TROP2$^{low/neg}$ cells and TROP2^{high} basal PESCs, whereas EPCAM$^-$ cells did not express TROP2, consistent with a stromal phenotype (Figure S1D and data not shown). Thus, magnetic-activated cell sorting (MACS) purification was used to enrich for EPCAM$^+$ cells to eliminate EPCAM$^-$ stromal cells and prevent fast overgrowth of the epithelial cells (Figures 1B, S1C, and S1D). Standard medium for primary PrECs (PrEGM; Lonza) was used with addition of the ROCK inhibitor Y-27632 in order to inhibit dissociation-induced apoptosis of epithelial cells (Liu et al., 2012; Zhang et al., 2011b). To further increase the specific plating efficiency of PESCs, as monitored by expression of CD49f and TROP2, we tested various culture surfaces. Although primary PrECs did not form significant numbers of colonies on standard culture flasks, significantly better attachment to hydrophobic surfaces was observed (Figures S1E and S1F). However, those conditions did not support proliferation, as cell numbers rapidly decreased within 5 days, indicating suboptimal culture conditions. Therefore, we next optimized the culture medium by including supplements that were previously used to expand embryonic stem cells (ESCs) and induced pluripotent stem cells (iPSCs) (Chen et al., 2011). We used combinatorial analyses of stem cell media components to design a novel "mouse prostate medium" (MPM) that supports the growth of primary murine PrECs. This medium contains Advanced Dulbecco's modified Eagle's medium (DMEM)/F12 supplemented with additional glutamine, glucose, EGF, bFGF, IGF-I, transferrin, and insulin (Figure S1G; Experimental Procedures).

After digestion of the murine prostate into single cells, enrichment using EPCAM-MACS, and growth of cells on hydrophobic surface flasks using MPM, the PrECs enriched for SCA-1$^+$CD49f$^+$TROP2^{high} basal PESCs and could be stably expanded for more than 30 passages ex vivo (Figure 1C). To examine whether the fast dominance of SCA-1$^+$CD49f$^+$TROP2^{high} cells was caused by their superior survival in these culture conditions, we determined apoptosis by staining for AnnexinV and propidium iodide (PI). Indeed, differentiated TROP2^{low} cells underwent cell death, whereas TROP2^{high} basal epithelial PESCs survived and proliferated (Figure S2A).

In summary, the method presented here is a feeder-free culture method for the in vitro expansion and maintenance of primary murine basal PESCs with an SCA-1$^+$CD49f$^+$TROP2^{high} phenotype.

Differentiation Capacity of Murine Basal PESCs

Most basal PESCs that are highly enriched for SCA-1$^+$CD49f$^+$TROP2^{high} express the prostate basal cell markers tumor protein p63 (TP63) and cytokeratin 5 (CK5), whereas cytokeratin 8 (CK8) and androgen receptor (AR), which are typically found on differentiated luminal cells, are rarely expressed (Figure 2A). As all cells showed an

Figure 1. Isolation, Magnetic Separation, and Expansion of Primary Murine Basal PESCs In Vitro

(A) FACS characterization of murine prostate cells after primary dissociation into single cells and staining with SCA-1, CD49f, TROP2, and lin cocktail (Ter119/CD31/CD45). Expression of TROP2 on lin$^-$ cells was evaluated in relation to CD49f and SCA-1 expression.

(B) Epithelial enrichment using EPCAM-MACS. FACS analyses before and after enrichment; distribution of TROP2 in the EPCAM$^-$, EPCAM$^+$/SCA-1$^-$, and EPCAM$^+$/SCA-1$^+$ populations.

(C) Polychromatic plot of Sca-1/CD49f/TROP2 expression on cultured murine cells after first passage. Comparison of CD49f/TROP2 expression after the third and 30th passages in vitro.

See also Figure S1 and Table S1.

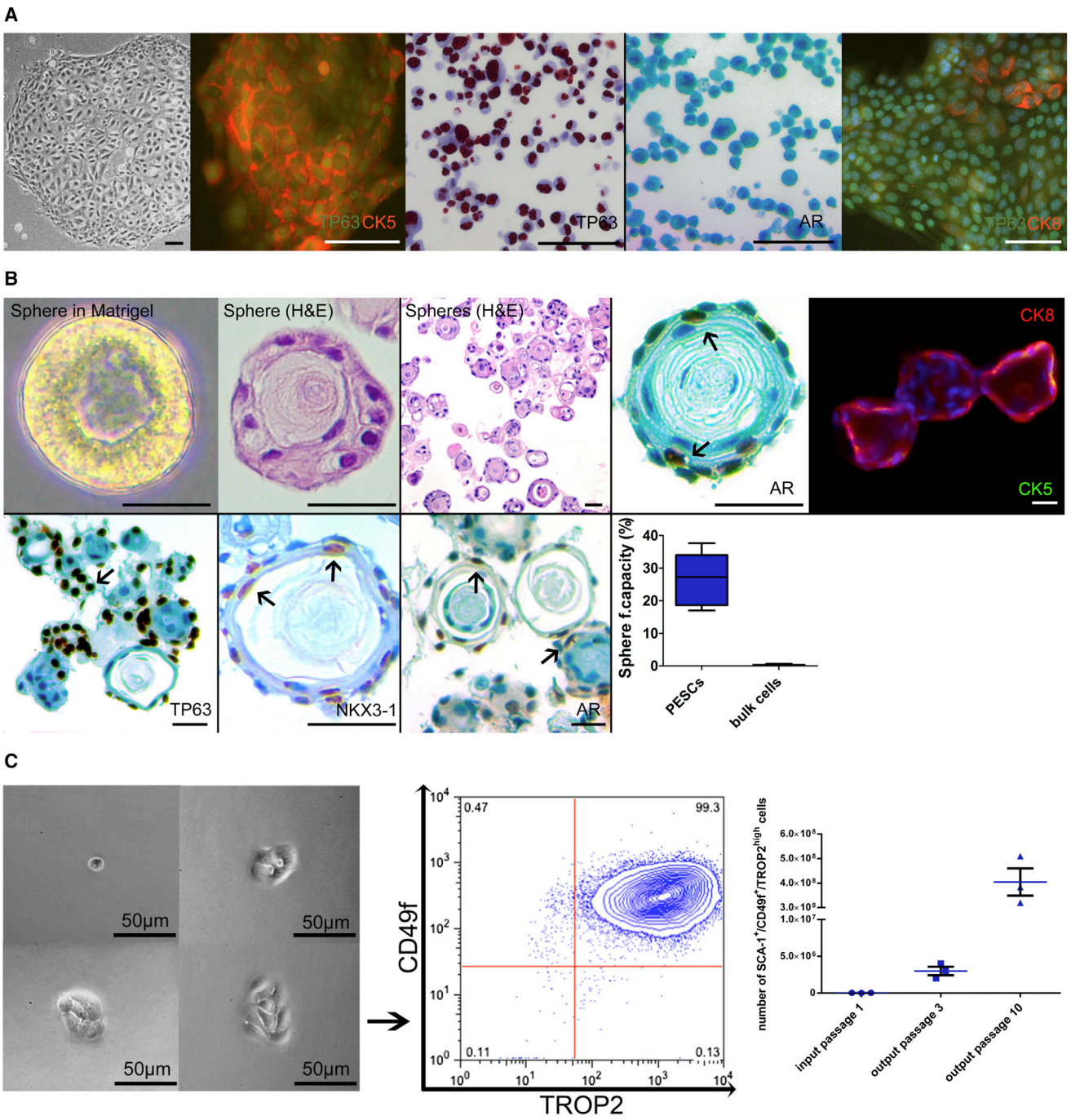

Figure 2. Characterization and Differentiation of Murine Basal PESCs

(A) IHC and immunofluorescence characterization of 2D cultured murine basal PESCs. Scale bar, 100 µm.

(B) Characterization of differentiated murine prostaspheres. Morphology in semisolid Matrigel; immunofluorescence and IHC of prostaspheres. Scale bar, 100 µm. For internal validation of TP63/AR/NKX3-1 antibodies, see Supplemental Experimental Procedures. The sphere-forming capacity of enriched PESCs was compared with bulk digested cells, n = 5 independent PESC preparations, $p < 0.01$ as determined by Student's two-tailed t test.

(C) In vitro self-renewal. Colonies derived from single-cell-sorted cultured PESCs retain their SCA-1^{+}/CD49f^{+}/TROP2^{high} phenotype after colony outgrowth. Amplification (cell numbers) of SCA-1^{+}/CD49f^{+}/TROP2^{high} cells using the MPM culture method, n = 3.

See also Figure S2 and Table S1.

almost uniform SCA-1$^+$CD49f$^+$TROP2^{high} PESC phenotype (Figure 1C), we tested their capacity to differentiate and self-renew in culture. For this purpose, the cells were transferred into semisolid growth conditions containing Matrigel and the formation of spheres was evaluated in comparison with unselected bulk prostate cells. The results show that 27% ± 7.4% of these cells had sphere-forming capacity (Figure 2B). Importantly, sphere formation was accompanied by a morphologic transition into organized epithelial tubule-like structures. The spheres resembled differentiated structures that retained TP63$^+$ basal cells as well as transit-amplifying cells, as indicated by co-expression of CK5 and CK8. In addition, spheres contained cells expressing AR and NKX3-1, consistent with a more differentiated luminal phenotype (Figure 2B). FACS analysis of spheres demonstrated the switch of CD49f$^+$/TROP2^{high} to a CD49f$^+$/TROP2^{low} phenotype, which is associated with the transition from a stem/progenitor to a more differentiated state (Goldstein et al., 2010). To address the capacity of those cells to serially form spheres, we sorted single CD49f$^+$/TROP2^{high} and CD49f$^+$/TROP2^{low} cells out of entire spheres and replated them in semisolid medium. As expected, only the CD49f$^+$/TROP2^{high} cells were able to serially form spheres and thus were the only cells with self-renewal activity (Figure S2B).

To address the self-renewal activity and proliferation of single sorted SCA-1$^+$CD49f$^+$TROP2^{high} cells, we regrew them in adherent cultures and evaluated their phenotype after colony outgrowth was observed. Almost all of the cells retained a SCA-1$^+$/CD49f$^+$/TROP2^{high} PESC phenotype. Additionally, the cells could be expanded to up to 4 × 10^8 cells in only ten passages (Figure 2C).

Human Basal PESCs Require Additional Progesterone and Sodium Selenite

After we established the primary murine PESC culture, we adapted the method to culture and expand PESCs isolated from human prostate. Single-cell suspensions of primary human prostate cells were obtained from patients with benign prostatic hyperplasia (BPH; Figure S3A). Subsequently, EPCAM$^+$ cells were enriched by MACS and cultured as described above for murine cells (MPM conditions). Since human cells did not expand at first, different culture surfaces were evaluated in conjunction with the addition of multiple stem cell media components. In contrast to mouse cells, human PrECs grew exclusively on BD Primaria surfaces, and not on hydrophobic surfaces (Figure 3A). Furthermore, addition of N2 supplement resulted in a significantly higher cell yield as compared with MPM alone (Figure 3B). Since the N2 supplement contains various components, we sought to further define the specific contribution of N2 ingredients. These experiments revealed that the combination of MPM plus progesterone and sodium selenite (termed human prostate medium [HPM]) is optimal for the outgrowth of primary human prostate epithelial colonies (Figure 3C). Cells that were enriched for the described human CD49f$^+$/TROP2^{high} basal PESC phenotype showed a high cloning efficiency (18% ± 2%) and expressed CK5 and TP63 as basal cell markers (Figures 3D and 3F). Similar to what was observed under the murine conditions, human PESCs could be stably expanded for more than 20 passages ex vivo, and cell numbers of up to 2.0 × 10^8 could be achieved after only eight passages (Figures 3E and S3B). Moreover, by transferring these cells into semisolid Matrigel, we were able to induce differentiation at a defined time point, resulting in a high sphere-forming capacity (20% ± 4%) and also demonstrating the capacity of a subset of cells to differentiate into CD49f$^+$/TROP2^{low} cells (Figures 3F and 3G; Goldstein et al., 2008). Using anti-human EPCAM$^+$ MACS enrichment followed by growth in Primaria flasks and HPM (plus ROCK inhibitor Y-27632), we were able to demonstrate the ex vivo expansion and maintenance of primary human basal PESCs in the absence of serum and feeder cells.

Primary Basal PESC Cultures Are Suitable for Medium- to High-Throughput Assays

To determine the genetic stability of PESC cultures, we performed karyotyping using multiplex fluorescence in situ hybridization (M-FISH) of human PESCs ex vivo. Karyotyping was performed on cultures of three different passage numbers, analyzing 15 individual metaphases each. This analysis confirmed a normal male karyotype (46,XY) (Figure 4A).

The establishment of primary basal PESC cultures grown as 2D adherent cells allowed us to evaluate whether the culture model is suitable for medium- to high-throughput assays. We thus expanded murine and human PESCs to 150 × 10^6 cells and performed 96-well-based screens to identify cell-surface markers for basal PESCs. Expression of 176 murine and 242 human cell-surface markers was tested on PESCs by flow cytometry (BD Lyoplate; data not shown). The results demonstrated the expression of previously described markers for basal PESCs, including CD29$^+$ and CD49f$^+$ (Goldstein et al., 2011). Moreover, all murine and human basal PESCs expressed high levels of CD24 (Figure S4). Expression of integrin alpha V (ITGAV) and integrin alpha-2 (ITGA2, CD49b) was validated by immunohistochemistry (IHC) on normal prostates, revealing a higher expression within the human prostate basal epithelial layer (Figures 4B and 4C; Collins et al., 2001; Liu and True, 2002). The screen also identified Syndecan-1 (SDC1) as a protein that is exclusively expressed in the human basal prostate compartment and not in differentiated luminal cells (Figure 4D). The identified cell-surface proteins may serve as a basis for future studies on basal PESCs

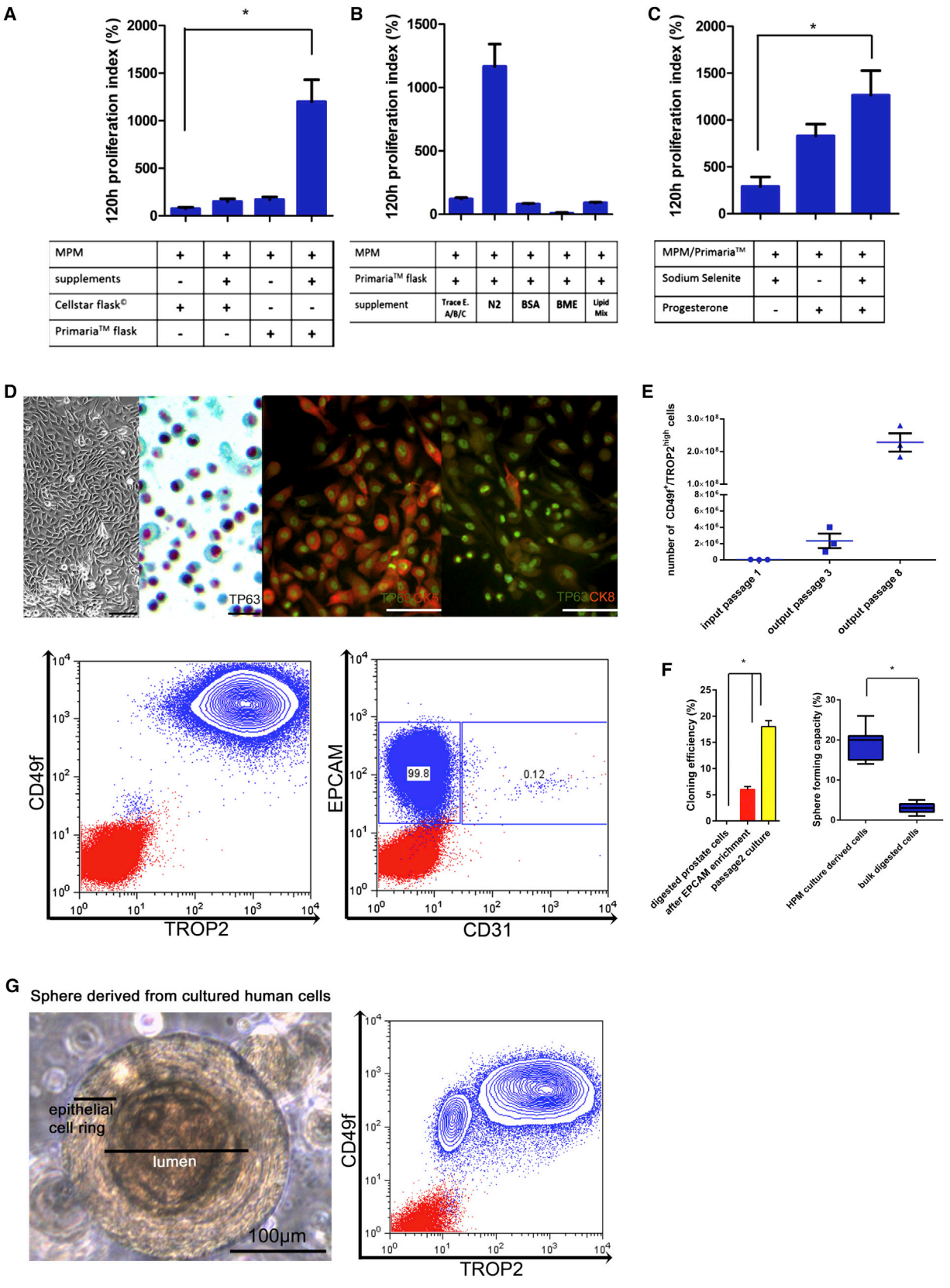

(legend on next page)

and confirm that our culture methods are suitable for medium- to high-throughput assays.

The Transcriptome of Murine and Human Basal PESCs Is Similar to That of ESCs

To uncover specific differences between basal PESCs and differentiated luminal cells, we compared the gene-expression profiles of mouse and human PESCs with profiles obtained from differentiated sphere cells. As the cultured cells were almost completely comprised of cells with an epithelial phenotype, we were able to establish pure expression profiles without contamination of profiles derived from other, non-epithelial cells of the prostate microenvironment (Figure 5A). Next, we performed gene set enrichment analyses (GSEAs) focusing primarily on gene sets enriched in both human and mouse basal PESCs with a false-discovery rate (FDR) < 0.001 (Mootha et al., 2003; Subramanian et al., 2005). This revealed distinct enrichment of specific gene sets in PESCs that are representative of immature pluripotent cells, especially ESC profiles (Figure 5B; Kesanakurti et al., 2013; Müller et al., 2008; Wong et al., 2008). Important regulators of stem cells and organogenesis, such as *SOX2*, *PRDX1*, *LMNB1*, and *PAK1*, showed a significantly higher mRNA expression in the undifferentiated PESC cultures (data not shown) (Kim et al., 2011; Yan et al., 2009; Zhang et al., 2011a; Zhu et al., 2009). We tested the levels of expression of human PRDX1 and PAK1 protein by IHC, which demonstrated that both proteins are expressed in the basal epithelial progenitor compartment (Figure S5A). Additionally, we identified LMNB1 (Lamin B1) as a putative new marker for PESCs, as we specifically detected expression within the basal compartment of the normal prostate as well as in cultured PESCs. In contrast, differentiated luminal cells in the prostate as well as in differentiated spheres did not express LMNB1 (Figure S5B).

GSEAs in Murine and Human PESCs Indicate Regulatory Roles of c-Myc and the TNFα/NF-kB Pathway

To identify potential signaling networks that maintain the undifferentiated versus differentiated state of basal PESCs, we performed GSEA focusing on gene sets that predict distinct transcription factor activities. This revealed upregulation of the *MYC* gene and multiple MYC targets in undifferentiated basal PESCs compared with differentiated sphere cells (Figure S6A). Moreover, during the process of differentiation into spheres, the PrECs showed a significant enrichment for TNFα- and NF-kB-mediated signaling cascades (Figure 6A). Enrichment plots of MYC targets and TNFα and NF-kB signaling suggest a possible regulatory network between the undifferentiated prostate basal stem cell state and more luminal differentiated spheres (Figure S6B). These results further reveal the upregulation of various signaling pathways in PESCs as compared with the more-differentiated sphere cells (Table S3).

Inhibition of NF-kB, but Not TNFα, Leads to Impaired Differentiation of Human PESCs

To test whether our culture platform is suitable for functional biological analyses, we focused on the postulated regulation of PESC differentiation into spheres by NF-kB or TNFα (Figure 6A). We transfected human PESCs of the CD49f^{+}/TROP2^{high} phenotype with a reporter construct to monitor the transcription factor NF-kB by expression of Venus (pV2b-NF-kB). Compared with the PESCs, more of the sphere cells expressed Venus. Moreover, Venus expression in human PESCs (HPM conditions) increased in response to stimulation by TNF-α (Figure 6B). This increase in NF-kB activity cannot be explained by the use of PrEGM and dihydrotestosterone (DHT), because PrEGM/DHT caused no increase of NF-kB activity alone

Figure 3. Adherent Enrichment and Expansion of Primary Human Basal PESCs In Vitro

(A–C) Combinatorial testing of factors for optimal expansion and enrichment of human PESCs. Starting with the defined MPM composition, the effect of different factors was determined by changes in the cell numbers after 120 hr (proliferation index 120 hr), n = 8 independent PESC preparations each. Statistical significance was evaluated by one-way ANOVA followed by Bonferroni post hoc tests, $p < 0.05$.

(A) Initial cell population after EPCAM enrichment and plating with ROCK inhibitor; additional supplementation of trace elements A/B/C, N2 supplement, BSA, BME, and lipid mix.

(B) Addition of N2 supplement to the MPM formulation is the main driver of proliferation for human basal PESCs.

(C) Progesterone and sodium selenite are the N2 constituents necessary for proliferation (HPM conditions).

(D) Micrographs, IHC, and immunofluorescence of cultured human basal PESCs, basal marker TP63, the luminal marker CK8, and the prostate cancer marker AMACR. Scale bars, 20 μm and 100 μM (for the immunofluorescence pictures). Flow-cytometric analyses of human basal PESCs at passage 5 for expression of CD49f, TROP2, EPCAM, and CD31.

(E) Amplification (cell numbers) of CD49f^{+}/TROP2^{high} cells using the HPM culture method; n = 3 independent PESC preparations.

(F) Cloning efficiency as determined by in vitro limiting dilution and Matrigel-sphere-forming capacity of human PESCs cultured under the final optimal conditions (Primaria surface and HPM); n = 5 independent PESC preparations, $p < 0.01$ as determined by Student's two-tailed t test.

(G) Morphology and expression of TROP2 and CD49f of differentiated human prostaspheres.

See also Figure S3 and Tables S1, S2, and S3.

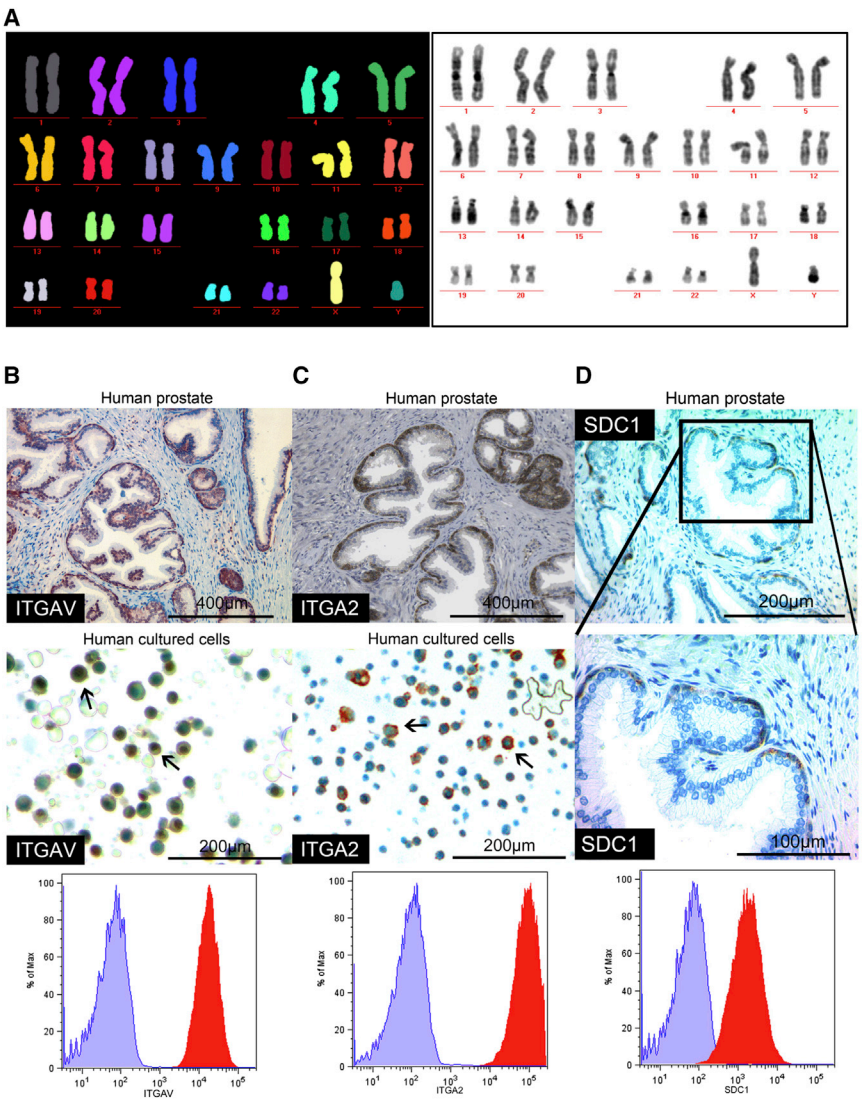

Figure 4. Genetic Stability of PESCs and Histologic Validation of FACS Array Screen-Identified Proteins in Human Prostate Glands

(A) M-FISH analysis of human PESCs in culture demonstrates a normal male karyogram (46,XY) with no signs of chromosomal aberrations; 24-color fluorophore-labeled metaphase chromosomes and their discrimination after visualization and computerized output.

(B and C) Staining for ITGAV and ITGA2 in primary human prostate and cultured human PESCs by IHC; surface expression on cultured human PESCs as determined by FACS.

(D) Exclusive expression of SDC1 in the human prostate basal epithelial compartment in vivo as determined by IHC. FACS surface staining of SDC1 in cultured human PESCs. The FACS plot shows the staining intensity for the isotype control (purple) and the specific antibody (red).

See also Figure S4.

(Figure 6B). Together, these results suggest that the observed NF-kB activation during the morphological transition into spheres is most likely due to the effect of differentiation itself and is consistent with the transcriptional activation of the NF-kB pathway during differentiation (Figures 6A and 6B). To determine whether the NF-kB pathway is important for differentiation into spheres, we blocked the pathway by the small-molecule inhibitor JSH-23, which inhibits NF-kB nuclear translocation, and assessed the sphere-forming capacity (Shin et al., 2004). JSH-23-treated cultures showed a significantly reduced sphere-forming capacity, whereas blocking of TNFα using the TNF-R2-Fc fusion protein Etanercept had no effect (Figure 6C). These data suggest that a TNFα-independent intrinsic or extrinsic mode of NF-kB activation is critically involved during sphere formation.

Cultured Basal PESCs Demonstrate Stem Cell Function In Vivo

In vivo transplantation assays are among the most commonly used methods for demonstrating stem cell activity. Such methods test the capacity of transplanted stem cells to generate and maintain entire tissue structures comprised of various differentiated cell types. Xin et al. (2003) previously demonstrated the regenerative capacity of the adult prostate epithelium in classical sandwich grafting experiments by co-transplanting prostate epithelium with fetal urogenital sinus mesenchyme (UGSM). These assays demonstrated that signals derived from the UGSM are required for the epithelial cells to generate prostate-gland-like structures in a transplant setting (Cunha and Lung, 1978; Goldstein et al., 2011; Lukacs et al., 2010). To test whether cultured cells retain functional stem cell

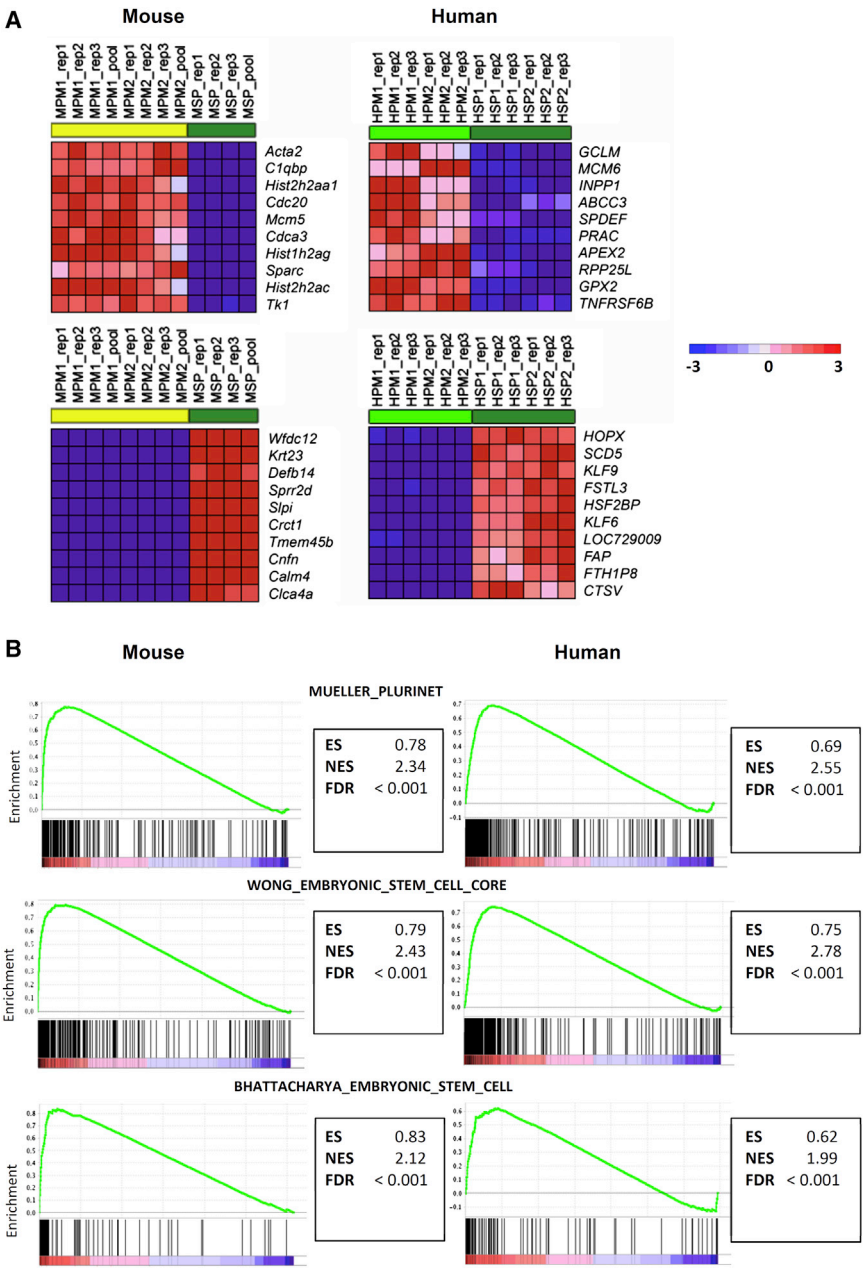

Figure 5. Cultured and Enriched PESCs Demonstrate Similarities to ESCs

(A) The top ten most differentially regulated genes in comparison with basal PESCs and the more differentiated sphere cells. Shown are the top ten upregulated genes in PESCs that are downregulated in spheres (upper two), as well as the top ten downregulated genes in PESCs that are upregulated in spheres (lower two). MPM, murine PESCs; MSP, murine spheres; HPM, human PESCs; HSP, human spheres.

(B) GSEA demonstrates enrichment of ESC gene signatures in undifferentiated cultured basal PESCs (Kesanakurti et al., 2013; Müller et al., 2008; Wong et al., 2008).

See also Figure S5.

activity, we lentivirally marked murine and human PESCs by concurrently introducing two fluorescent proteins, tdTomato and Venus (Weber et al., 2008, 2011; Figure S7A). Subsequent subcutaneous (s.c.) transplantation of LeGO-V2/T2 marked SCA-1^{+}CD49f^{+}TROP2^{high} mouse PESCs, which were mixed with unmarked E16 UGSM and revealed prostatic tubules after 10–12 weeks. Their PESC origin was confirmed by immunofluorescence imaging and anti-GFP IHC (Venus). As few as 10^4 mouse SCA-1^{+}CD49f^{+}TROP2^{high} PESCs were sufficient to induce growth of prostatic tubules when transplanted subcutaneously. Although no engraftment was observed when cells were transplanted intraprostatically (without UGSM), intermediate results were obtained by transplanting cells under the kidney capsule (with UGSM) (Figures 7A and 7B; Table S4). Importantly, new prostatic tubules derived from cultured mouse basal PESCs preserved TP63^{+} basal cells and demonstrated differentiated AR^{+}-expressing cells encircling the lumina of formed acini, confirming their typical 3D cellular structure at the molecular level.

As few as 100 cultured human basal PESCs were able to regenerate prostate acini in nude mice (Figures 7D and

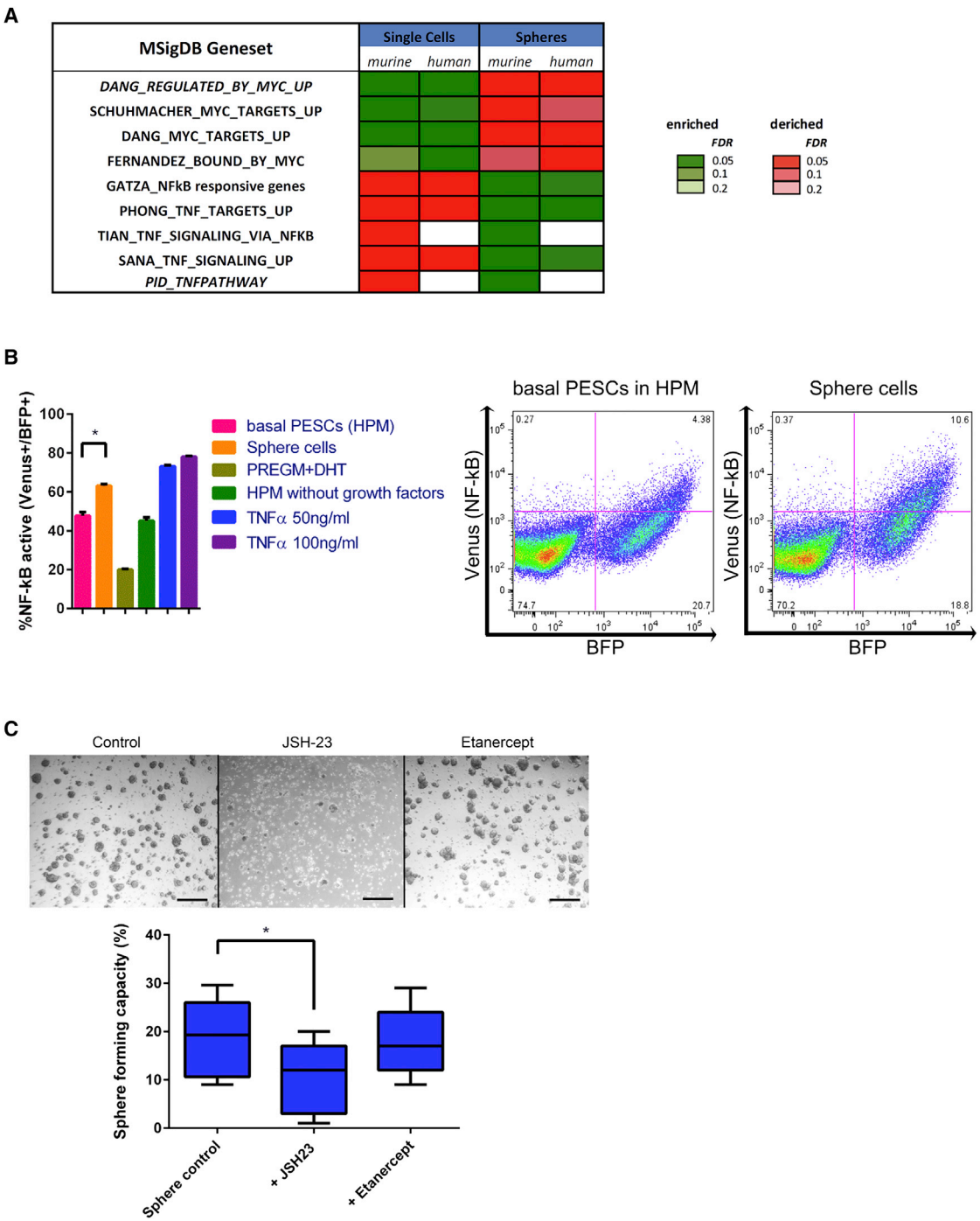

Figure 6. GSEAs Indicate a Functional Role of NF-kB/TNFα in Undifferentiated and Differentiated States of Basal PESCs

(A) Significantly changed gene sets (GSEA) in undifferentiated basal PESCs as compared with differentiated prostasphere cells (Subramanian et al., 2005; Zutter and Santoro, 1990).

(B) FACS analyses of NF-kB transcriptional reporter activity in human cells (left, n = 5 independent PESC preparations, statistical significance was evaluated by one-way ANOVA followed by Bonferroni post hoc tests, $p < 0.05$), % NF-kB active = % Venus/BFP positivity in FITC/Pacific blue cytometer channels and two corresponding FACS plots, demonstrating NF-kB activity in basal PESCs in HPM conditions as compared with increased NF-kB activity in differentiated sphere cells (right).

(legend continued on next page)

A

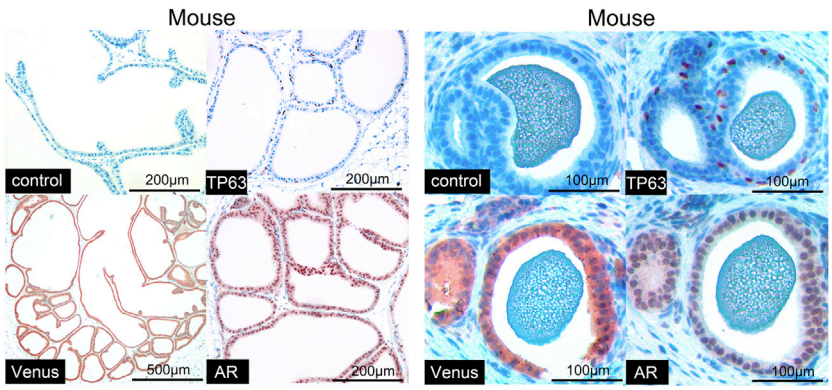

B

No.CD49f^{+}/TROP2^{high}	Nude mice	NOD/SCID mice
1x10^{3}	**0/5**	**0/10**
1x10^{4}	**6/10**	**3/10**
1x10^{5}	**1/10**	**1/10**
0.5x10^{6}	**8/10**	**2/10**
1x10^{6}	**4/5**	

C

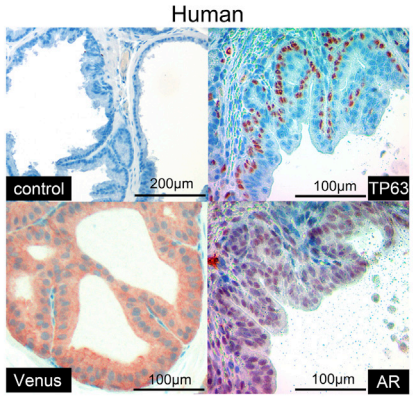

D

No.CD49f^{+}/TROP2^{high}	Nude mice	NOD/SCID mice
1x10^{2}	**4/10**	**0/5**
1x10^{3}	**2/10**	**1/5**
1x10^{4}	**0/10**	**0/5**
1x10^{5}	**5/10**	**0/5**
5x10^{5}	**8/10**	**2/5**

Figure 7. Cultured and Enriched Basal PESCs Preserve Functional Adult Stem Cell Capacity In Vivo

(A) Formation of prostate gland-like acini after s.c. transplantation of cultured Venus^{+} murine PESCs together with unmarked E16 UGSM. Immunohistochemical staining for TP63 and AR. Venus was detected with an anti-GFP antibody.

(B) Frequency of murine prostate acini regeneration in a limiting-dilution in vivo transplantation assay.

(C) Prostate-gland-like acini formation after s.c. transplantation of cultured Venus^{+} human PESCs together with unmarked E16 UGSM. Immunohistochemical staining for TP63, AR, and Venus (anti-GFP).

(D) Frequency of human prostate acini regeneration in a limiting-dilution in vivo transplantation assay.

See also Figure S7 and Table S4.

S7B; Table S4). For both human and mouse PESCs, nude mice represented the more efficient recipients compared with the more immune-compromised NOD/SCID mice. Regenerated human prostate acini were built up of a single TP63^{+} basal cell layer and single or multiple layers of differentiated AR^{+} luminal cells, closely resembling the microscopic anatomy of normal human prostate epithelium (Figures 7C and S7C). In summary, our results demonstrate that cultured murine as well as human primary PESCs are able to regenerate entire prostatic acini, demonstrating that these cells have adult prostate stem cell activity in vivo.

DISCUSSION

Here, we provide a novel method to expand and study functional basal PESCs in adherent cultures. Simple serum- and feeder-free conditions were established to

(C) Inhibition of NF-kB leads to impaired differentiation of human PESCs. Micrographs and corresponding sphere-forming-capacity results of PESCs seeded into regular sphere conditions (PrEGM/Matrigel = sphere control) in comparison with sphere conditions with the addition of NF-kB inhibitor JSH-23 or Etanercept to block soluble TNFα-mediated TNFR binding (n = 5 independent PESC preparations each; statistical significance was evaluated by one-way ANOVA followed by Bonferroni post hoc tests, $p < 0.05$).

See also Figure S6 and Table S3.

grow and expand murine Lin^{neg}CD49f^{+}SCA-1^{+}TROP2^{high} and human Lin^{neg}CD49f^{+}TROP2^{high} PESCs. The reported method represents a major advance from previous protocols (Goldstein et al., 2011; Lukacs et al., 2010; Rhim et al., 2011; Robinson et al., 1998) and complements the protocol recently proposed by Karthaus et al. (2014) to expand and maintain enriched prostate progenitor cells ex vivo. The method also overcomes the presence of undefined media and culture components such as bovine pituitary extract (Peehl and Stamey, 1986). The ability to significantly expand functional human basal PESCs, in terms of both total number and frequency, will help investigators overcome the bottleneck related to the limited availability of primary prostate patient tissue for cellular, molecular, genomic, and pharmacological analyses.

A key element of the culture conditions is the balanced combination of growth factors and signaling molecules (e.g., EGF, bFGF, IGF, insulin, transferrin, and Rock inhibitor), which apparently generates an artificial androgen-independent PESC microenvironment that promotes the self-renewal and maintenance of 2prostate stem cell fate. Although these factors have been known for a long time in the cell-culture field, it was critical to discover the exact composition of the media in combination with a hydrophobic surface that would allow significant expansion of undifferentiated murine basal PESCs as compared with the widely used standard method (PrEGM). The necessary adaptations to enable human basal PESC amplification included the switch to surface-treated flasks and the addition of sodium selenite and progesterone. Progesterone has also been reported to induce mammary epithelial progenitor cell expansion, indicating that it may promote hormone-controlled epithelial stem cells in general (Joshi et al., 2010). Expanded basal PESCs not only show expression signatures similar to those of pluripotent ESCs and other somatic stem cells but also harbor functional stem cell potential, as demonstrated by their capacity to generate prostatic tubules in vivo. These results are comparable to those obtained in transplantation experiments performed with PESCs isolated from primary prostate biopsies (Goldstein et al., 2010, 2011; Lukacs et al., 2010). The method described here now allows the robust expansion of such primary cells and thus facilitates an in-depth analysis of the molecular programs employed.

One can induce expanded PESCs to differentiate at any desired time point by transferring the cells from adherent conditions into previously described prostasphere culture conditions (Xin et al., 2007). However, the described method cannot be used to study the role of luminal PESCs, which have also been reported to be a self-sustaining lineage (Karthaus et al., 2014). In addition to basal PESCs, luminal PESCs have also been suggested to be the putative cell of origin for prostate cancer (Choi et al., 2012; Goldstein et al., 2010; Wang et al., 2009). Furthermore, in vitro differentiation into spheres can only a serve as a model system and does not resemble the full luminal differentiation program of prostate gland development in vivo. This limitation and the putative presence of transit-amplifying (intermediate) cells have to be considered when using these methods (Ousset et al., 2012; Pastrana et al., 2011). Additionally, the methods we have described for murine cells cannot be used to replace lineage-tracing mouse models—they can only complement the findings from such models. In particular, work by Wang et al. (2013) clearly shows that prostate basal cells develop a substantial plasticity ex vivo when they are removed from their normal environment. In line with this, our experiments confirm the finding that a significant discrepancy exists between the high in vitro sphere-forming capacity of basal PESCs and their capacity to form glands in vivo. In vivo, only a small proportion of basal cells were shown to have a graft-regenerating capacity (Wang et al., 2013). Nevertheless, our methods additionally facilitate the analysis of primary human cells, allowing such cells to be amplified, manipulated, and studied in detail. Clearly, the direct analysis of human cells holds the potential to provide data that are of more relevance to the biology of human development and disease.

The culture method described here creates a novel platform for studying prostate disease etiology and progression. PESCs grown as adherent feeder-free cultures are easy to manipulate (e.g., for transfection and infection) and can be induced to differentiate or transplanted to form prostate tubules in vivo. Thus, this method will provide the basis for various in-depth analyses of epithelial prostate stem cells. First, it provides the basis to selectively expand and study murine basal PESCs isolated from different genetically engineered mice, such as in the PTEN prostate cancer model (Di Cristofano et al., 2001). This may help to identify molecular mechanisms during differentiation and the progression from normal prostate basal stem cells to hyperplastic and possibly even neoplastic epithelium (Carver et al., 2011). However, one has to keep in mind that prostate cancers that arise from basal stem cells may have a different phenotype and clinical outcome compared with those derived from luminal prostate stem cells (Choi et al., 2012; Lu et al., 2013). Second, using co-culture techniques that combine basal PESCs with cellular prostate stromal components (e.g., associated fibroblasts and smooth muscle cells), one can dissect and study important cross regulations between primary PESCs and their corresponding microenvironmental niche to better understand prostate-gland regulation at a more global level. Third, human basal PESCs isolated from patients with BPH can be isolated and studied at the molecular and genomic levels, and subsequently linked to their

biologic behavior in vitro and in vivo. An estimated 50% of men show histologic evidence of BPH by the age of 50 years, and 40%–50% of these men become clinically significant, demonstrating the clinical relevance of this novel method. Finally, mouse- or patient-derived and expanded PESCs can be used for high-throughput screens using knockdown or chemical compound libraries. This novel mouse and human method to expand functional PESCs may boost research on normal prostate gland biology and may open up new possibilities for studying the etiology of prostatic diseases.

EXPERIMENTAL PROCEDURES

Prostate Cell Preparation and Identification of Basal/Luminal Prostate Epithelial Cells by Flow Cytometry

Microdissection, enzymatic digestion, and preparation of single cells from male C57Bl/6 mice prostate primary human prostate were performed as described previously (Goldstein et al., 2011; Lukacs et al., 2010). We changed the described enzymatic digestion of the human prostate into a 4 hr routine to obtain higher cell yields (specific steps are provided in Supplemental Experimental Procedures). For isolation of primary human cells from surgical prostate tissues, we obtained informed consent according to the principles of the Declaration of Helsinki. Procedures were approved by the responsible ethics committee of Heidelberg University (permit S-479/2009). For detailed information regarding patient tissues, see Table S2. Identification of basal stem cells by the lineage^{neg} (Ter119$^-$/CD31$^-$/CD45$^-$) SCA-1$^+$CD49f$^+$TROP2^{high} phenotype in the murine prostate, as well as the CD49f$^+$TROP2^{high} phenotype in the human prostate, was performed as described previously (Goldstein et al., 2008, 2010; Lukacs et al., 2010; Xin et al., 2005). CD49f$^+$TROP2^{low} cells have been identified and characterized before as more differentiated epithelial phenotype cells (Goldstein et al., 2008, 2010, 2011). Please see Table S5 for specific antibody information. We began our new enrichment and culture methods after enzymatic digestion of the primary murine or human prostate into single cells.

Adherent Expansion of Primary Murine and Human Basal PESCs

As a combined first step in establishing the murine and human cell cultures, we performed MACS enrichment for EPCAM$^+$ cells after primary preparation of single-cell suspensions from murine and human prostates (Figure 1). For this purpose, we stained digested murine cell suspensions with anti-mouse CD326 (EPCAM)-phycoerythrin (PE) (Clone 8.8; eBioscience) followed by indirect magnetic bead labeling using anti-PE microbeads (Miltenyi Biotec). For human cells, we directly used anti-human EPCAM microbeads (Miltenyi Biotec) according to the manufacturer's instructions. Magnetic enrichment was performed using the autoMACS Pro Separator (Miltenyi Biotec). We altered the tissue culture flask surfaces by comparing negatively charged standard plastic culture flasks (TPP) with hydrophobic (suspension) culture flasks (Cellstar; Greiner Bio-One) or net-negative pretreated surface flasks (Primaria; BD). After evaluating the appropriate culture surface, we tested different combinations of stem cell media components (described in detail in Figures 1, 2, 3, and S1 and Table S1). Cells were plated in either hydrophobic CellStar (Greiner) 24-well plates (murine) or 24-well Primaria (BD) plates (human) with individual combinations of media components (n = 8). We evaluated the proliferation index by evaluating the cell number at a specific time point divided by the number of input cells at time zero. The best media for the expansion of murine prostate basal epithelial progenitor cells, MPM, consists of Advanced DMEM/F12 supplemented with additional glutamine, glucose, EGF, bFGF, LONG R^3 IGF-I, holo-transferrin, and insulin. The best media for the expansion of human prostate basal epithelial progenitor cells, HPM, is the MPM formulation plus additional progesterone and sodium selenite.

Prostasphere Assay and Analysis/Sorting of Sphere-Derived Single Cells

The semisolid prostasphere assay used for in vitro differentiation analyses has been described elsewhere (Xin et al., 2007). Briefly, cultured murine or human prostate basal epithelial cells were resuspended in a 50:50 mixture of Matrigel (BD) and PrEGM (Lonza) and plated around the rim of a well of a 12-well tissue culture plate. The Matrigel mix was allowed to solidify at 37°C and then 800 µl PrEGM was added. To recover the sphere cells for subsequent flow-cytometry analysis/cell sorting, we used Cell Retrieval Solution (BD) followed by sphere digestion into single cells using StemPro-Accutase (GIBCO) in combination with mechanical trituration using a 27-gauge needle and 40-µm filters.

Flow Cytometry and Single-Cell-Sorting Experiments

All cell sortings were performed on BD FACS Aria II or Aria III cell sorters. To minimize loss of cell viability, we performed experiments on fresh cell suspensions out of our culture, prepared shortly before flow cytometry, detaching the cells using StemPro-Accutase (GIBCO). Antibody staining was performed in PBS supplemented with 5 mM EDTA. Please see Table S5 for specific antibody information. Prior to flow cytometry or sorting, cells were filtered using 40-µm filters. The sorting buffer included PBS, 5 mM EDTA and 10 µM Y-27632 ROCK inhibitor (Tocris Bioscience). Forward-scatter height (FSC-H) versus forward-scatter width (FSC-W), and side-scatter height (SSC-H) versus side-scatter width (SSC-W) profiles were used to eliminate cell doublets. Dead cells were eliminated by excluding PI$^+$ cells, whereas contaminating human or mouse Lin$^+$ cells were eliminated by gating on Ter119/CD31/CD45-FITC$^-$ for mouse and CD45/CD3-FITC$^-$ for human cells. Gates for FACS experiments were determined by using isotype controls for the respective specific antibodies used. Gates were then set to exclude the respective population in the isotype control experiment. In single-cell-sorting experiments, each cell was individually sorted into a different well of a 96-well plate, using a built-in protocol in the FACS Aria II and III software packages, with appropriate adjustments (device: 96-well plate, precision: single-cell). For sorting, we used a 100-µm nozzle. Sorted single cells were additionally evaluated by microscopy. We assessed the true clonogenicity of single basal progenitor cell-derived colonies quantitatively by performing a limiting-dilution analysis in vitro using 96-well plates and L-Calc software (Stem-Cell Technologies)

after observing colony outgrowth and confirming a stable SCA-1^{+}/CD49f^{+}/TROP2^{high} phenotype.

Lentiviral Vectors and Lentiviral Gene Transfer

LeGO-V2 (Venus) and LeGO-T2 (tdTomato) were previously described (Weber et al., 2011) and kindly provided by Kristoffer Weber and Boris Fehse. Lentiviral particles were generated as previously described (Kutner et al., 2009). For transduction, prostate cells were cultured in MPM or HPM for 24 hr at a fixed cell number. Target cells were incubated in the presence of 8 μg ml^{-1} polybrene for 12 hr at 37°C with viral supernatant at a multiplicity of infection (moi) of 50–60 per vector. Transduction efficiency was validated 48–72 hr after transduction using FACS.

Mouse Experiments and Evaluation of In Vivo Stem Cell Capability

All mouse experiments were approved by the animal-protection officers of the German Cancer Research Center (DKFZ) and the state of Baden-Württemberg in accordance with German law (Tierschutzgesetz, G18-12). Male NOD-SCID and nude mice were bred at the animal facility of the DKFZ and maintained under pathogen-free, individual ventilated-cage conditions. E16 UGSM was used for co-injections with culture-derived prostate progenitor cells to provide the necessary growth signals to promote in vivo prostate gland regeneration. Before performing the co-injections, we prepared the UGSM according to previously described protocols (Lukacs et al., 2010). First, we set up timed pregnancies in C57Bl/6 mice and harvested the fetuses at day 16 of pregnancy. We cut the fetus in half below the liver and microdissected the pelvic UGSM under the stereomicroscope while placing the bottom half of the fetus in a supine position and holding the hind legs apart with forceps (Cunha and Lung, 1978). The UGSM was removed and separated intact by gently pulling up on the bladder. To prove the in vivo stem cell capability of our culture-derived cells, we co-injected our LeGO-V2/T2 marked cultured murine or human cells together with E16 UGSM and Matrigel into male nude or NOD/SCID mice subcutaneously into the renal capsule, as well as intraprostatically (without UGSM). For detailed information, see Figure 7 and Table S4. Experimental results were obtained using passage 5 (early) cultured cells, though engraftment could also be observed using late passage numbers (data not shown). To support differentiation, we subcutaneously implanted testosterone pellets (12.5 mg/90-day release; Innovative Research of America). After 10–12 weeks, we harvested the regenerated s.c. grafts for subsequent analyses. Before conducting histological analyses on fixed tissue, we visualized direct Venus fluorescence in freshly dissected s.c. grafts under the fluorescent stereomicroscope.

IHC and Immunofluorescence

For IHC of differentiated spheres, we retrieved prostaspheres from the Matrigel using Cell Retrieval Solution (BD). The spheres were then fixed in 10% buffered formalin and transferred into HistoGel (Thermo Scientific) for subsequent sectioning and staining with various antibodies according to the manufacturer's instructions. Antibodies for basal epithelial TP63 and differentiated luminal epithelial markers (AR, NKX3-1) were validated on primary prostate tissue before use (for detailed analyses, see Supplemental Experimental Procedures). For immunofluorescence, cells were grown in Cellstar (Greiner Bio-One) or BD Primaria six-well plates, fixed within the wells using BD Cytofix for 30 min at 4°C, and stained overnight with primary antibodies. The next day, staining was done with secondary anti-IgG-Alexa 488 (Invitrogen) and anti-IgG-Alexa 546 (Invitrogen). Finally, cells were counterstained with ProLong antifade reagent (Invitrogen) and visualized with a standard fluorescence microscope. Please see Table S5 for specific IHC and immunofluorescence antibody information. Regenerated s.c. tissue grafts were fixed in 10% buffered formalin and placed in 70% ethanol. Sections (4 μm) were stained with hematoxylin and eosin (H&E) or rabbit polyclonal anti-GFP/Venus antibody (ab290; Abcam). We previously validated the antibody for detection of Venus to prove the in vivo stem cell capability of our culture-derived cells as compared with coinjected untransduced cells of the fetal urogenital sinus.

ACCESSION NUMBERS

The expression array data reported in this work have been deposited in the Gene Expression Omnibus under accession number GSE61861.

SUPPLEMENTAL INFORMATION

Supplemental Information includes Supplemental Experimental Procedures, seven figures, and five tables and can be found with this article online at http://dx.doi.org/10.1016/j.stemcr.2015.01.015.

AUTHOR CONTRIBUTIONS

T.H. developed the methods and designed the study, performed culture and differentiation experiments in vitro and in vivo, and wrote the manuscript. C.E. helped with lentiviral constructs and performed bioinformatics analyses. C.K. performed experiments and supervised all mouse transplantation experiments. T.R.-W., S.W., and E.N. helped with vector design and experiments. S.M.-G., V.V., and W.W. performed histological analyses and secondary pathologic evaluations. A.J. and B.S. performed M-FISH analyses. I.B., A.S., and S.P. analyzed the data and/or provided intellectual guidance regarding their interpretation. M.R.S. and A.T. designed the study, analyzed and evaluated results, and wrote the manuscript. All authors read and approved the final version of the manuscript.

ACKNOWLEDGMENTS

We thank Dr. S. Schmitt and his team at the DKFZ Flow Cytometry Core Facilities for expert technical assistance, and Dr. M. Milsom for discussions and critical reading of the manuscript. We also thank Dr. B. Fehse (University Medical Center Hamburg-Eppendorf) for providing LeGO constructs. This work was supported by the BioRN Spitzencluster "Molecular and Cell Based Medicine," supported by the German Bundesministerium für Bildung und Forschung (BMBF), the SFB 873 "Maintenance and Differentiation of Stem Cells in Development and Disease" funded by the Deutsche Forschungsgemeinschaft (DFG), and the Dietmar-Hopp Foundation.

Received: June 26, 2014
Revised: January 18, 2015
Accepted: January 19, 2015
Published: February 19, 2015

REFERENCES

Carver, B.S., Chapinski, C., Wongvipat, J., Hieronymus, H., Chen, Y., Chandarlapaty, S., Arora, V.K., Le, C., Koutcher, J., Scher, H., et al. (2011). Reciprocal feedback regulation of PI3K and androgen receptor signaling in PTEN-deficient prostate cancer. Cancer Cell *19*, 575–586.

Chaproniere, D.M., and McKeehan, W.L. (1986). Serial culture of single adult human prostatic epithelial cells in serum-free medium containing low calcium and a new growth factor from bovine brain. Cancer Res. *46*, 819–824.

Chen, G., Gulbranson, D.R., Hou, Z., Bolin, J.M., Ruotti, V., Probasco, M.D., Smuga-Otto, K., Howden, S.E., Diol, N.R., Propson, N.E., et al. (2011). Chemically defined conditions for human iPSC derivation and culture. Nat. Methods *8*, 424–429.

Choi, N., Zhang, B., Zhang, L., Ittmann, M., and Xin, L. (2012). Adult murine prostate basal and luminal cells are self-sustained lineages that can both serve as targets for prostate cancer initiation. Cancer Cell *21*, 253–265.

Collins, A.T., Habib, F.K., Maitland, N.J., and Neal, D.E. (2001). Identification and isolation of human prostate epithelial stem cells based on alpha(2)beta(1)-integrin expression. J. Cell Sci. *114*, 3865–3872.

Cunha, G.R., and Lung, B. (1978). The possible influence of temporal factors in androgenic responsiveness of urogenital tissue recombinants from wild-type and androgen-insensitive (Tfm) mice. J. Exp. Zool. *205*, 181–193.

Di Cristofano, A., De Acetis, M., Koff, A., Cordon-Cardo, C., and Pandolfi, P.P. (2001). Pten and p27KIP1 cooperate in prostate cancer tumor suppression in the mouse. Nat. Genet. *27*, 222–224.

Evans, G.S., and Chandler, J.A. (1987). Cell proliferation studies in the rat prostate: II. The effects of castration and androgen-induced regeneration upon basal and secretory cell proliferation. Prostate *11*, 339–351.

Goldstein, A.S., Lawson, D.A., Cheng, D., Sun, W., Garraway, I.P., and Witte, O.N. (2008). Trop2 identifies a subpopulation of murine and human prostate basal cells with stem cell characteristics. Proc. Natl. Acad. Sci. USA *105*, 20882–20887.

Goldstein, A.S., Huang, J., Guo, C., Garraway, I.P., and Witte, O.N. (2010). Identification of a cell of origin for human prostate cancer. Science *329*, 568–571.

Goldstein, A.S., Drake, J.M., Burnes, D.L., Finley, D.S., Zhang, H., Reiter, R.E., Huang, J., and Witte, O.N. (2011). Purification and direct transformation of epithelial progenitor cells from primary human prostate. Nat. Protoc. *6*, 656–667.

Joshi, P.A., Jackson, H.W., Beristain, A.G., Di Grappa, M.A., Mote, P.A., Clarke, C.L., Stingl, J., Waterhouse, P.D., and Khokha, R. (2010). Progesterone induces adult mammary stem cell expansion. Nature *465*, 803–807.

Kabalin, J.N., Peehl, D.M., and Stamey, T.A. (1989). Clonal growth of human prostatic epithelial cells is stimulated by fibroblasts. Prostate *14*, 251–263.

Karthaus, W.R., Iaquinta, P.J., Drost, J., Gracanin, A., van Boxtel, R., Wongvipat, J., Dowling, C.M., Gao, D., Begthel, H., Sachs, N., et al. (2014). Identification of multipotent luminal progenitor cells in human prostate organoid cultures. Cell *159*, 163–175.

Kesanakurti, D., Chetty, C., Rajasekhar Maddirela, D., Gujrati, M., and Rao, J.S. (2013). Essential role of cooperative NF-κB and Stat3 recruitment to ICAM-1 intronic consensus elements in the regulation of radiation-induced invasion and migration in glioma. Oncogene *32*, 5144–5155.

Kim, Y., Sharov, A.A., McDole, K., Cheng, M., Hao, H., Fan, C.M., Gaiano, N., Ko, M.S., and Zheng, Y. (2011). Mouse B-type lamins are required for proper organogenesis but not by embryonic stem cells. Science *334*, 1706–1710.

Klinger, R.Y., Blum, J.L., Hearn, B., Lebow, B., and Niklason, L.E. (2006). Relevance and safety of telomerase for human tissue engineering. Proc. Natl. Acad. Sci. USA *103*, 2500–2505.

Kogan, I., Goldfinger, N., Milyavsky, M., Cohen, M., Shats, I., Dobler, G., Klocker, H., Wasylyk, B., Voller, M., Aalders, T., et al. (2006). hTERT-immortalized prostate epithelial and stromal-derived cells: an authentic in vitro model for differentiation and carcinogenesis. Cancer Res. *66*, 3531–3540.

Kutner, R.H., Zhang, X.Y., and Reiser, J. (2009). Production, concentration and titration of pseudotyped HIV-1-based lentiviral vectors. Nat. Protoc. *4*, 495–505.

Litvinov, I.V., Vander Griend, D.J., Xu, Y., Antony, L., Dalrymple, S.L., and Isaacs, J.T. (2006). Low-calcium serum-free defined medium selects for growth of normal prostatic epithelial stem cells. Cancer Res. *66*, 8598–8607.

Liu, A.Y., and True, L.D. (2002). Characterization of prostate cell types by CD cell surface molecules. Am. J. Pathol. *160*, 37–43.

Liu, X., Ory, V., Chapman, S., Yuan, H., Albanese, C., Kallakury, B., Timofeeva, O.A., Nealon, C., Dakic, A., Simic, V., et al. (2012). ROCK inhibitor and feeder cells induce the conditional reprogramming of epithelial cells. Am. J. Pathol. *180*, 599–607.

Lu, T.L., Huang, Y.F., You, L.R., Chao, N.C., Su, F.Y., Chang, J.L., and Chen, C.M. (2013). Conditionally ablated Pten in prostate basal cells promotes basal-to-luminal differentiation and causes invasive prostate cancer in mice. Am. J. Pathol. *182*, 975–991.

Lukacs, R.U., Goldstein, A.S., Lawson, D.A., Cheng, D., and Witte, O.N. (2010). Isolation, cultivation and characterization of adult murine prostate stem cells. Nat. Protoc. *5*, 702–713.

Miki, J., and Rhim, J.S. (2008). Prostate cell cultures as in vitro models for the study of normal stem cells and cancer stem cells. Prostate Cancer Prostatic Dis. *11*, 32–39.

Mootha, V.K., Lindgren, C.M., Eriksson, K.F., Subramanian, A., Sihag, S., Lehar, J., Puigserver, P., Carlsson, E., Ridderstråle, M., Laurila, E., et al. (2003). PGC-1alpha-responsive genes involved in oxidative phosphorylation are coordinately downregulated in human diabetes. Nat. Genet. *34*, 267–273.

Morrison, S.J., and Spradling, A.C. (2008). Stem cells and niches: mechanisms that promote stem cell maintenance throughout life. Cell *132*, 598–611.

Müller, F.J., Laurent, L.C., Kostka, D., Ulitsky, I., Williams, R., Lu, C., Park, I.H., Rao, M.S., Shamir, R., Schwartz, P.H., et al. (2008). Regulatory networks define phenotypic classes of human stem cell lines. Nature *455*, 401–405.

Ousset, M., Van Keymeulen, A., Bouvencourt, G., Sharma, N., Achouri, Y., Simons, B.D., and Blanpain, C. (2012). Multipotent and unipotent progenitors contribute to prostate postnatal development. Nat. Cell Biol. *14*, 1131–1138.

Pastrana, E., Silva-Vargas, V., and Doetsch, F. (2011). Eyes wide open: a critical review of sphere-formation as an assay for stem cells. Cell Stem Cell *8*, 486–498.

Peehl, D.M., and Stamey, T.A. (1986). Growth responses of normal, benign hyperplastic, and malignant human prostatic epithelial cells in vitro to cholera toxin, pituitary extract, and hydrocortisone. Prostate *8*, 51–61.

Rhim, J.S., Li, H., and Furusato, B. (2011). Novel human prostate epithelial cell culture models for the study of carcinogenesis and of normal stem cells and cancer stem cells. Adv. Exp. Med. Biol. *720*, 71–80.

Robinson, E.J., Neal, D.E., and Collins, A.T. (1998). Basal cells are progenitors of luminal cells in primary cultures of differentiating human prostatic epithelium. Prostate *37*, 149–160.

Shin, H.M., Kim, M.H., Kim, B.H., Jung, S.H., Kim, Y.S., Park, H.J., Hong, J.T., Min, K.R., and Kim, Y. (2004). Inhibitory action of novel aromatic diamine compound on lipopolysaccharide-induced nuclear translocation of NF-kappaB without affecting IkappaB degradation. FEBS Lett. *571*, 50–54.

Stoyanova, T., Goldstein, A.S., Cai, H., Drake, J.M., Huang, J., and Witte, O.N. (2012). Regulated proteolysis of Trop2 drives epithelial hyperplasia and stem cell self-renewal via β-catenin signaling. Genes Dev. *26*, 2271–2285.

Subramanian, A., Tamayo, P., Mootha, V.K., Mukherjee, S., Ebert, B.L., Gillette, M.A., Paulovich, A., Pomeroy, S.L., Golub, T.R., Lander, E.S., and Mesirov, J.P. (2005). Gene set enrichment analysis: a knowledge-based approach for interpreting genome-wide expression profiles. Proc. Natl. Acad. Sci. USA *102*, 15545–15550.

Visvader, J.E. (2011). Cells of origin in cancer. Nature *469*, 314–322.

Wang, X., Kruithof-de Julio, M., Economides, K.D., Walker, D., Yu, H., Halili, M.V., Hu, Y.P., Price, S.M., Abate-Shen, C., and Shen, M.M. (2009). A luminal epithelial stem cell that is a cell of origin for prostate cancer. Nature *461*, 495–500.

Wang, Z.A., Mitrofanova, A., Bergren, S.K., Abate-Shen, C., Cardiff, R.D., Califano, A., and Shen, M.M. (2013). Lineage analysis of basal epithelial cells reveals their unexpected plasticity and supports a cell-of-origin model for prostate cancer heterogeneity. Nat. Cell Biol. *15*, 274–283.

Weber, K., Bartsch, U., Stocking, C., and Fehse, B. (2008). A multicolor panel of novel lentiviral "gene ontology" (LeGO) vectors for functional gene analysis. Mol. Ther. *16*, 698–706.

Weber, K., Thomaschewski, M., Warlich, M., Volz, T., Cornils, K., Niebuhr, B., Täger, M., Lütgehetmann, M., Pollok, J.M., Stocking, C., et al. (2011). RGB marking facilitates multicolor clonal cell tracking. Nat. Med. *17*, 504–509.

Wong, D.J., Liu, H., Ridky, T.W., Cassarino, D., Segal, E., and Chang, H.Y. (2008). Module map of stem cell genes guides creation of epithelial cancer stem cells. Cell Stem Cell *2*, 333–344.

Wu, C.T., Altuwaijri, S., Ricke, W.A., Huang, S.P., Yeh, S., Zhang, C., Niu, Y., Tsai, M.Y., and Chang, C. (2007). Increased prostate cell proliferation and loss of cell differentiation in mice lacking prostate epithelial androgen receptor. Proc. Natl. Acad. Sci. USA *104*, 12679–12684.

Xin, L., Ide, H., Kim, Y., Dubey, P., and Witte, O.N. (2003). In vivo regeneration of murine prostate from dissociated cell populations of postnatal epithelia and urogenital sinus mesenchyme. Proc. Natl. Acad. Sci. USA *100* (*Suppl 1*), 11896–11903.

Xin, L., Lawson, D.A., and Witte, O.N. (2005). The Sca-1 cell surface marker enriches for a prostate-regenerating cell subpopulation that can initiate prostate tumorigenesis. Proc. Natl. Acad. Sci. USA *102*, 6942–6947.

Xin, L., Lukacs, R.U., Lawson, D.A., Cheng, D., and Witte, O.N. (2007). Self-renewal and multilineage differentiation in vitro from murine prostate stem cells. Stem Cells *25*, 2760–2769.

Yan, Y., Sabharwal, P., Rao, M., and Sockanathan, S. (2009). The antioxidant enzyme Prdx1 controls neuronal differentiation by thiol-redox-dependent activation of GDE2. Cell *138*, 1209–1221.

Zhang, H., Landmann, F., Zahreddine, H., Rodriguez, D., Koch, M., and Labouesse, M. (2011a). A tension-induced mechanotransduction pathway promotes epithelial morphogenesis. Nature *471*, 99–103.

Zhang, L., Valdez, J.M., Zhang, B., Wei, L., Chang, J., and Xin, L. (2011b). ROCK inhibitor Y-27632 suppresses dissociation-induced apoptosis of murine prostate stem/progenitor cells and increases their cloning efficiency. PLoS ONE *6*, e18271.

Zhu, S., Wurdak, H., Wang, J., Lyssiotis, C.A., Peters, E.C., Cho, C.Y., Wu, X., and Schultz, P.G. (2009). A small molecule primes embryonic stem cells for differentiation. Cell Stem Cell *4*, 416–426.

Zutter, M.M., and Santoro, S.A. (1990). Widespread histologic distribution of the alpha 2 beta 1 integrin cell-surface collagen receptor. Am. J. Pathol. *137*, 113–120.

Stem Cell Reports, Volume *4*

Supplemental Information

Defined Conditions for the Isolation and Expansion of Basal Prostate Progenitor Cells of Mouse and Human Origin

Thomas Höfner, Christian Eisen, Corinna Klein, Teresa Rigo-Watermeier, Stephan M. Goeppinger, Anna Jauch, Brigitte Schoell, Vanessa Vogel, Elisa Noll, Wilko Weichert, Irène Baccelli, Anja Schillert, Steve Wagner, Sascha Pahernik, Martin R. Sprick, and Andreas Trumpp

Figure S1, related to Figure 1

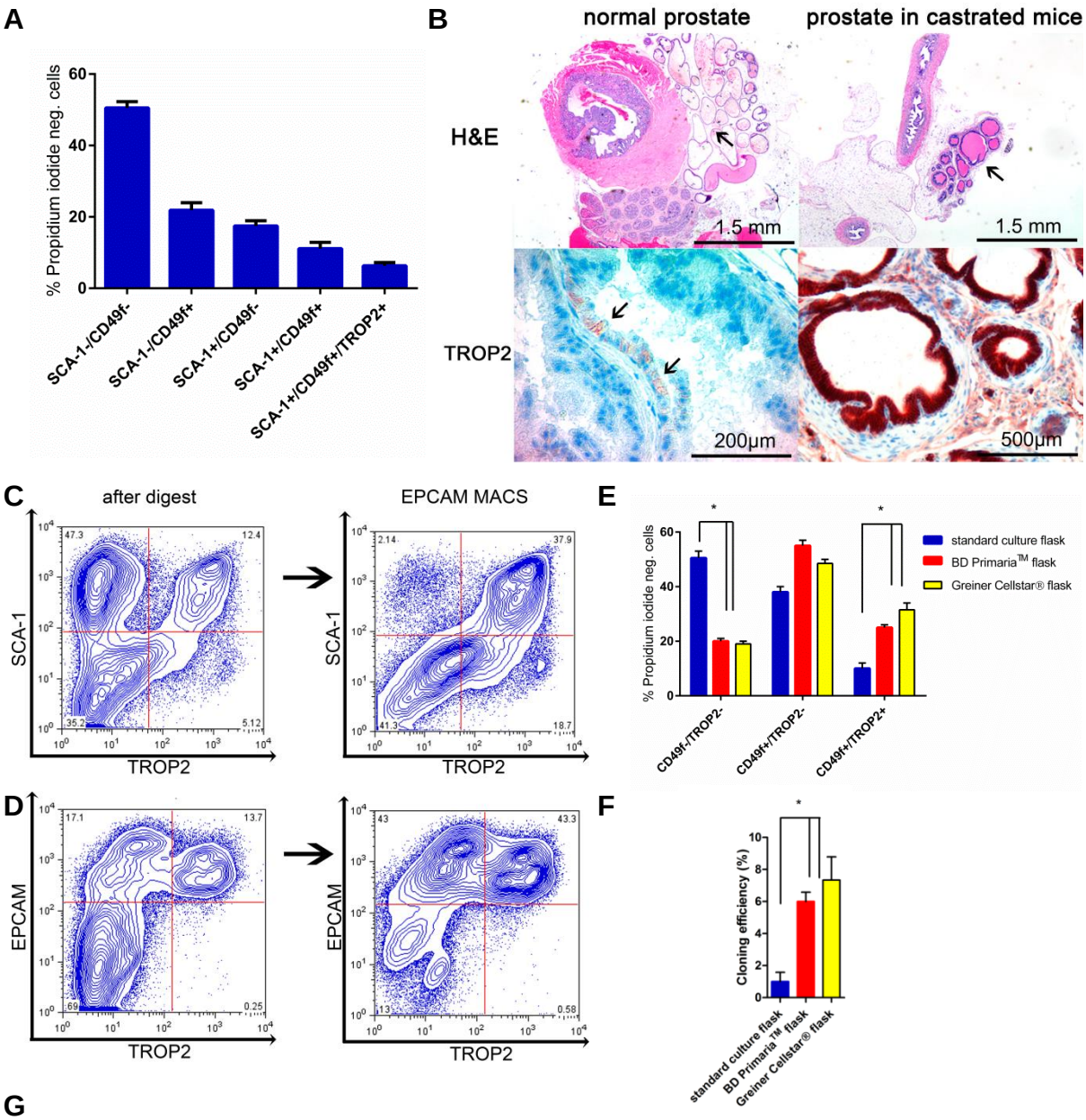

G

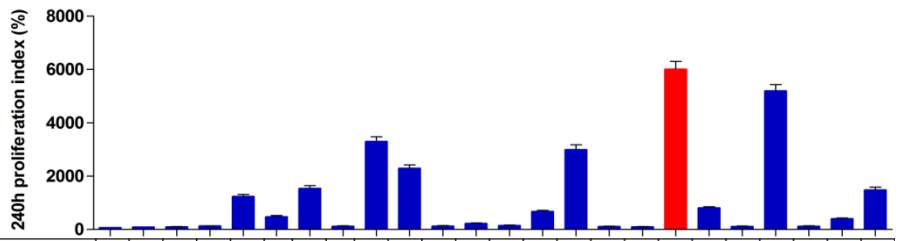

Glucose	-	-	-	+	-	-	-	-	-	+	+	+	+	+	+	+	+	+	+	+	+	+	+	+
EGF	-	-	-	-	+	-	+	-	+	+	-	-	-	+	+	-	-	+	+	-	+	-	-	-
bFGF	-	-	-	-	-	+	+	-	+	+	-	-	-	+	+	-	-	+	+	-	+	-	-	-
IGF1R3	-	-	-	-	-	-	-	+	+	+	-	-	-	-	-	-	-	+	+	-	+	-	-	-
N2 supplement	-	-	-	-	-	-	-	-	-	-	-	-	-	-	-	-	+	-	-	+	+	-	-	-
Transferrin	-	-	-	-	-	-	-	-	-	-	+	-	+	-	-	-	-	+	-	-	-	+	-	-
Insulin	-	-	-	-	-	-	-	-	-	-	-	+	+	-	-	-	-	+	-	-	-	+	-	-
BME	-	-	-	-	-	-	-	-	-	-	-	-	-	+	+	-	-	-	-	-	-	-	-	-
BSA	-	-	-	-	-	-	-	-	-	-	-	-	-	+	-	+	-	-	+	+	-	+	-	-
FCS	-	-	-	-	-	-	-	-	-	-	-	-	-	-	-	-	-	-	-	-	-	-	+	-
BPE	-	-	-	-	-	-	-	-	-	-	-	-	-	-	-	-	-	-	-	-	-	-	-	+
A.DMEM/F12 + Glutamine	-	-	+	+	+	+	+	+	+	+	+	+	+	+	+	+	+	+	+	+	+	+	+	+
A.DMEM/F12	-	+	-	-	-	-	-	-	-	-	-	-	-	-	-	-	-	-	-	-	-	-	-	-
PREGM	+	-	-	-	-	-	-	-	-	-	-	-	-	-	-	-	-	-	-	-	-	-	-	-

Figure S1, related to Figure 1

Characterization of purification and culture conditions of murine basal PESCs

(A) Characterization of murine prostate cells after primary prostate digest. Initial flow cytometry analyses of murine prostate cells after primary prostate digest, FACS gating on viable (PI^-), lineage Ter119/CD31/CD45 neg. cells, n=5, Error bars, SD. **(B)** TROP2 is expressed by few prostate epithelial cells and a marker for basal epithelial progenitor cells. Histological comparisons between prostates of 16 week old C57Bl/6 WT mice with prostates of 16 week old C57Bl/6 castrated mice (androgen withdrawel), left and right images, arrows point at epithelial glands. Prostates in castrated mice demonstrate general atrophy. The epithelium reacts with luminal atrophy and basal cell hyperplasia (arrow upper right image)(Reuter, 1997). TROP2 staining in prostates of castrated mice recapitulate enhanced epithelial progenitor specific TROP2 positivity compared to TROP2 expression in normal prostates (lower images, basal progenitor cell hyperplasia in castrated mice) (Goldstein et al., 2008). **(C) (D)** EPCAM MACS enrichment efficiency to preselect for epithelial specific $TROP2^{low+high}$ cells. SCA-1/TROP2 and EPCAM/TROP2 expressions by FACS before and after EPCAM MACS. FACS gating on PI^-, lin^- cells. $TROP2^+$ cells are a distinct subpopulation of $SCA\text{-}1^+$ cells within the prostate (only ¼ of all $SCA\text{-}1^+$ cells are $TROP2^+$). The $EPCAM^+$ epithelial fraction within the prostate contains the distinct subpopulation of basal PESCs ($TROP2^{high}$) and more differentiated epithelial cells ($TROP2^{low}$) demonstrating an approximate 1:1 ratio (Goldstein et al., 2010). This ratio can be maintained after EPCAM MACS enrichment. **(E) (F)** Enhanced adhesion/cloning efficiency of murine basal PESCs on hydrophobic surface. Enhanced adhesion (S1E) and cloning efficiency (S1F) of basal PESCs using either surface modified polystyrene (BD Primaria™) or hydrophobic surface flasks (Greiner Cellstar), 3 days after EPCAM-MACS, with ROCK inhibitor and standard PrEGM media, n=8 independent PESC preparations. Error bars, SD. Asterisk (∗) indicates statistical significance by one-way ANOVA followed by Bonferroni post hoc tests; $p< 0.05$. **(G)** Defining essential media components for primary murine basal PESCs. Dissection of growth factors needed to expand and maintain undifferentiated murine basal PESCs *in vitro*. Cell proliferation was measured at different time points and 240 h after EPCAM-MACS and plating in hydrophobic surface flasks with ROCK inhibitor; $p< 0.001$ as calculated by one-way ANOVA followed by Bonferroni post hoc tests; n=8 independen PESC preparations. The proliferation index represents the cell

number at a specific time point divided by the number of input cells at time 0. Error bars, SD (MPM media conditions).

Figure S2, related to Figure 2

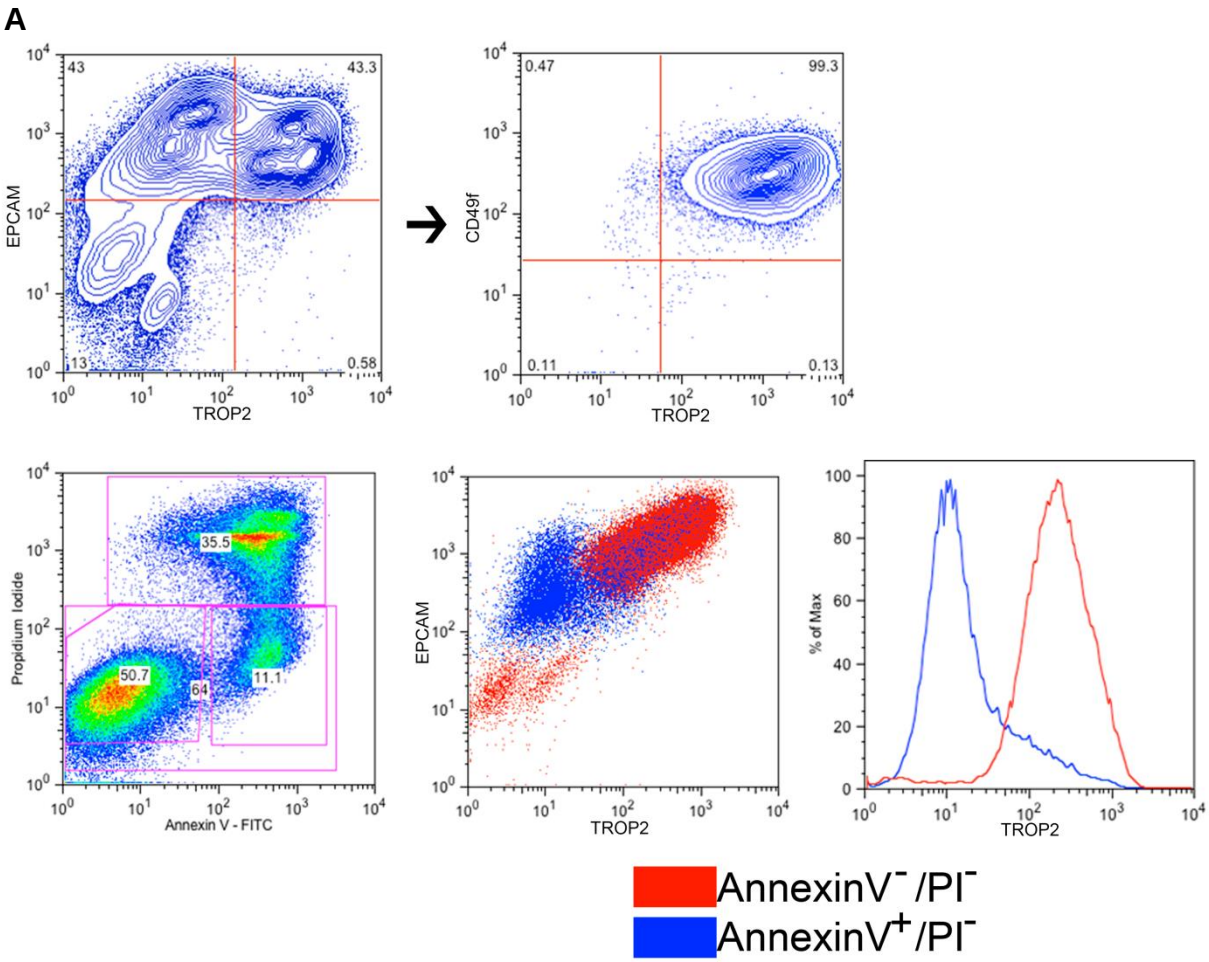

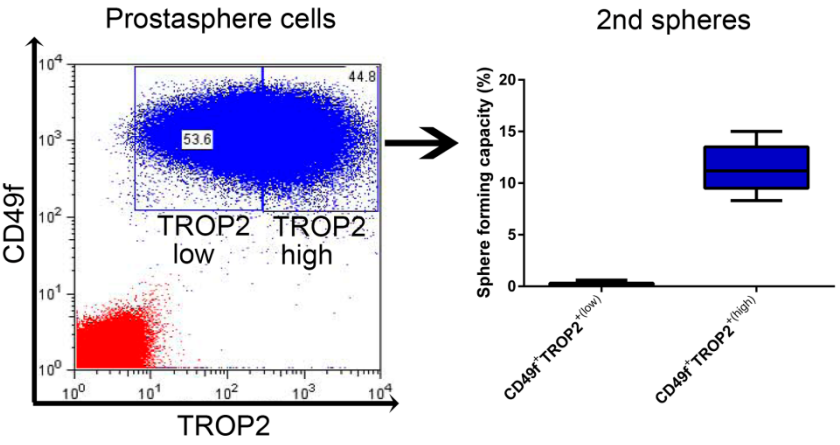

Figure S2, related to Figure 2

Enrichment and sphere forming capacity of murine basal PESCs *in vitro*

(A) Enrichment of basal prostate epithelial stem cell phenotype *in vitro* is based on the proliferation of EPCAM^{+}/TROP2^{high} basal cells while EPCAM^{+}/TROP2^{low} cells become apoptotic. Enrichment of PESCs *in vitro* (upper FACS plots). AnnexinV/Propidium iodide staining of murine prostate cells shortly (3 days) after initial plating in ideal culture conditions (MPM + hydrophobic CellStar flask, lower FACS plots). **(B)** Serial sphere forming capacity of murine prostasphere cells. Flow cytometry of prostasphere cells (in semisolid matrigel) derived from single cell sorted cultured cells (passage 5, left image). After murine prostasphere formation CD49f^{+}/ TROP2^{high} and CD49f^{+}/TROP2^{low} cells were sorted and replated in matrigel. Serial sphere forming capacity of sorted prostasphere cells (right image), n=8 independent PESC preparations.

Figure S3, related to Figure 3

A

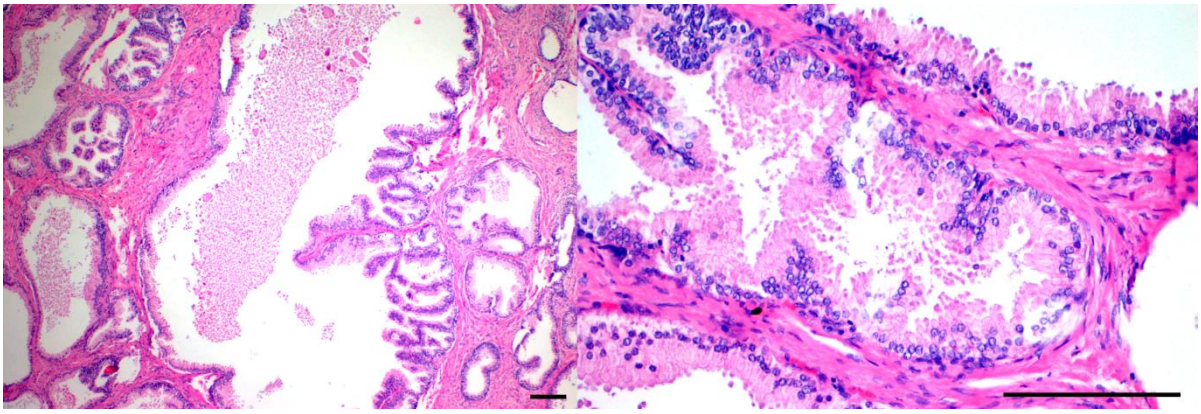

B

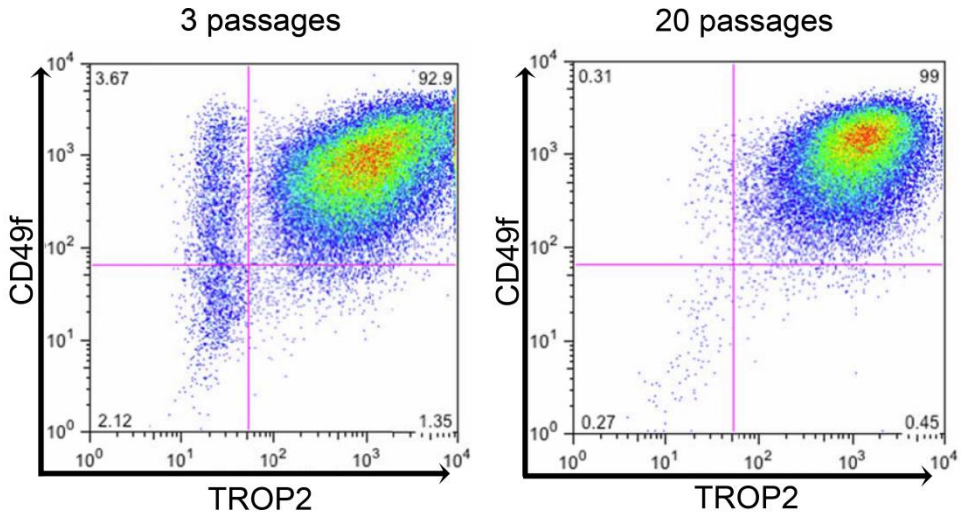

Figure S3, related to Figure 3

Patient derived PESCs can be enriched and expanded using HPM conditions

(A) Patient derived benign prostatic hyperplasia, from which PESCs were enriched and expanded using HPM conditions. H&E staining examples of patient prostate histology, from which tissue was obtained. Scale bar = 200µm. For detailed patient information see Table S2. **(B)** Human PESCs can be expanded for more than 20 passages and retain the CD49f/TROP2 phenotype. FACS plots demonstrating the $CD49f^{+}/TROP2^{high}$ phenotype of human PESCs in passage 3 and passage 20 using HPM conditions.

Figure S4, related to Figure 4

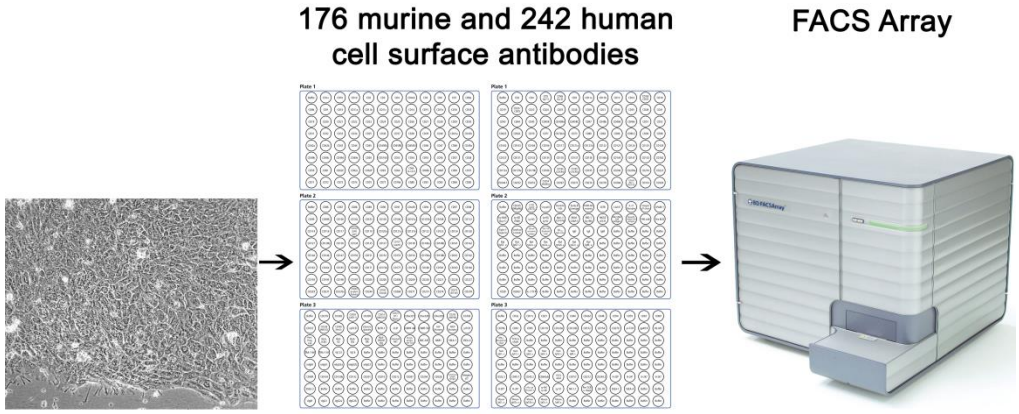

Results of murine cell surface protein array

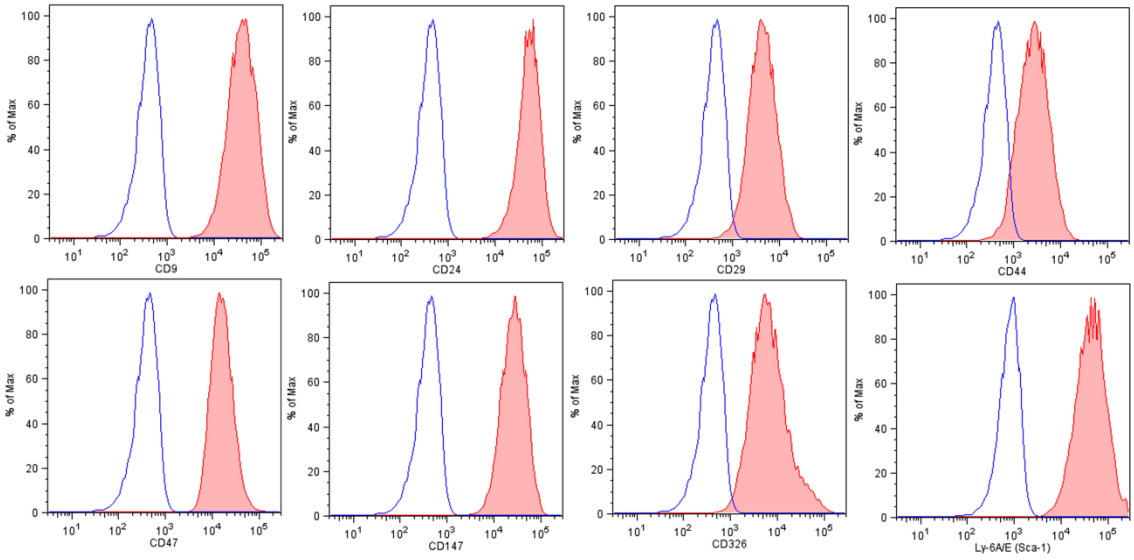

Corresponding results in human cell surface protein array

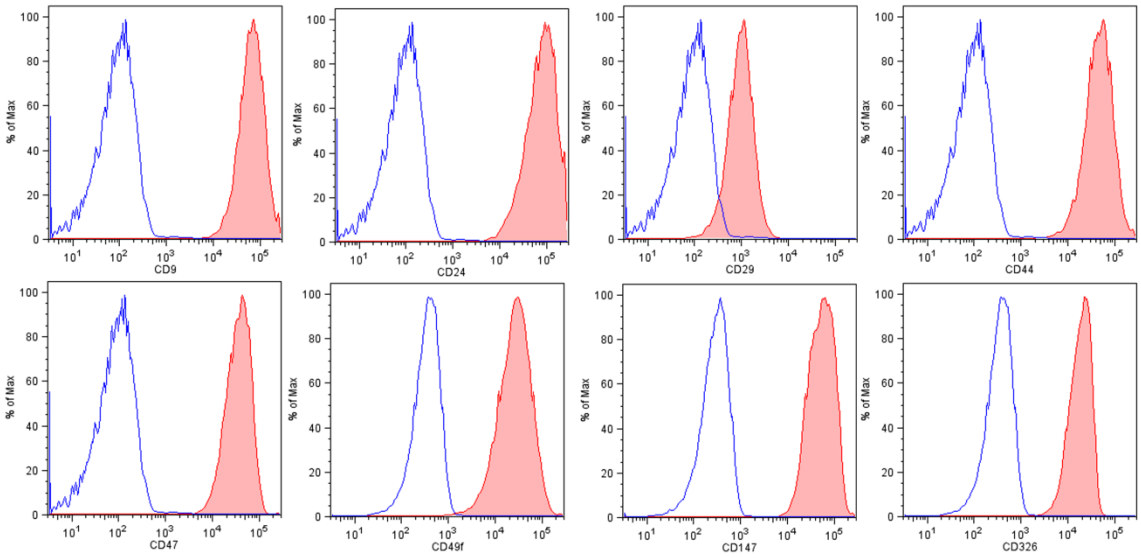

Figure S4, related to Figure 4

Cell surface protein profiling of murine and human prostate basal epithelial progenitor cells

Examples of surface protein expression results of murine as well as human PESCs using a flow cytometry high-throughput screening (BD FACSArray™ Bioanalyzer) after staining with 242 anti-human monoclonal antibodies or 176 anti-mouse monoclonal antibodies using BD Lyoplate™ Cell Surface Marker Screening Panels; blue cell populations=corresponding isotype controls; red cell populations=protein stainings (Alexa 647); final analysis by FlowJo software, Tree Star, Inc.

Figure S5, related to Figure 5

A

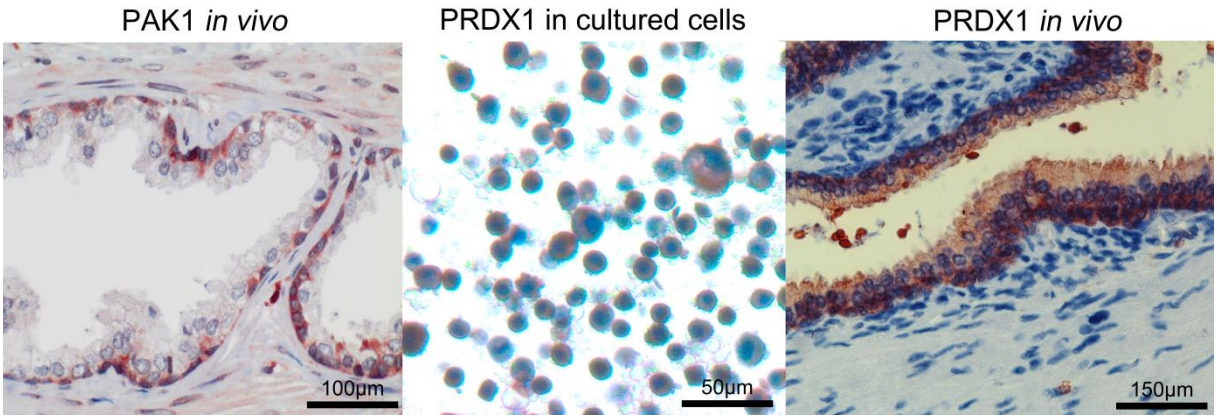

B

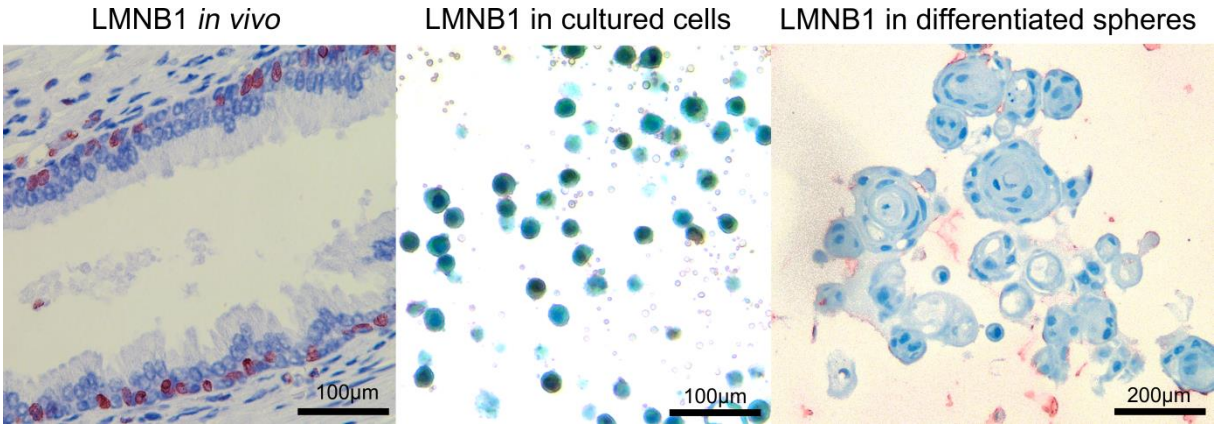

Figure S5, related to Figure 5

Corresponding IHC protein expressions of highly upregulated progenitor related genes

(A) Expression of PAK1 and PRDX1 in the human prostate epithelial compartment. Corresponding IHC protein expressions of highly upregulated progenitor related genes *PAK1* and *PRDX1* in basal PESCs as discovered by gene expression analysis. Graphs demonstrate that PAK1 and PRDX1 are expressed in the human prostate basal compartment of primary human prostate. Staining of PRDX1 in cultured basal PESCs (middle). **(B)** LMNB1 (Lamin B1) as a putative new marker for human basal PESCs. Corresponding IHC protein expression of highly upregulated progenitor related gene *LMNB1* in primary human prostate tissue *in vivo* and in cultured human PESCs *in vitro.* Downregulation of expression in differentiated prostaspheres *in vitro*.

Figure S6, related to Figure 6

A

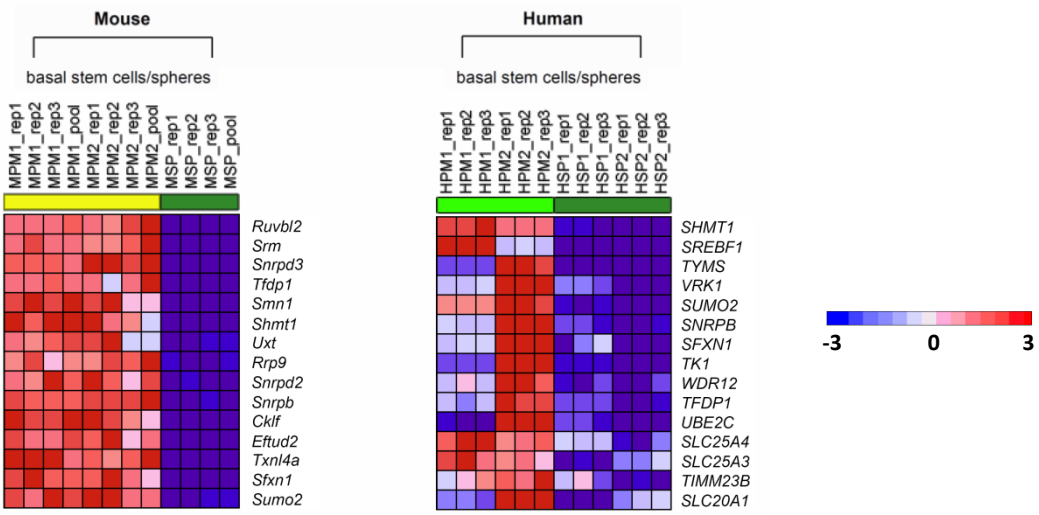

B

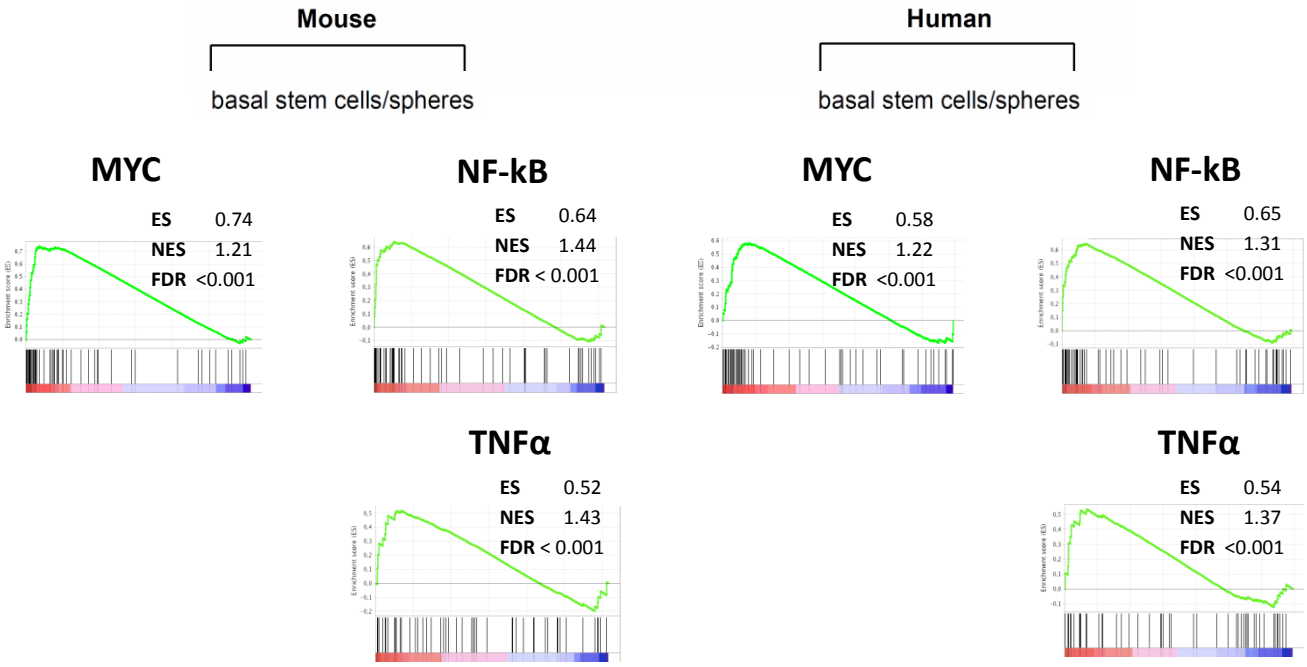

Figure S6, related to Figure 6

GSE analyses indicate involvement of MYC/NF-kB/TNFα pathways in undifferentiated and differentiated states of basal PESCs

(A) Upregulation of multiple known MYC target genes in cultured basal PESCs as compared to differentiated prostasphere cells. **(B)** Enrichment plots of MYC target genes in cultured basal PESCs as well as enrichment plots of TNFα and NF-kB pathway genes in differentiated spheres. GSEA enrichment plots indicating upregulation of MYC targets in undifferentiated PESCs whereas genes involved in the NF-kB and TNFα pathways are upregulated in the more differentiated sphere cells.

Figure S7, related to Figure 7

A

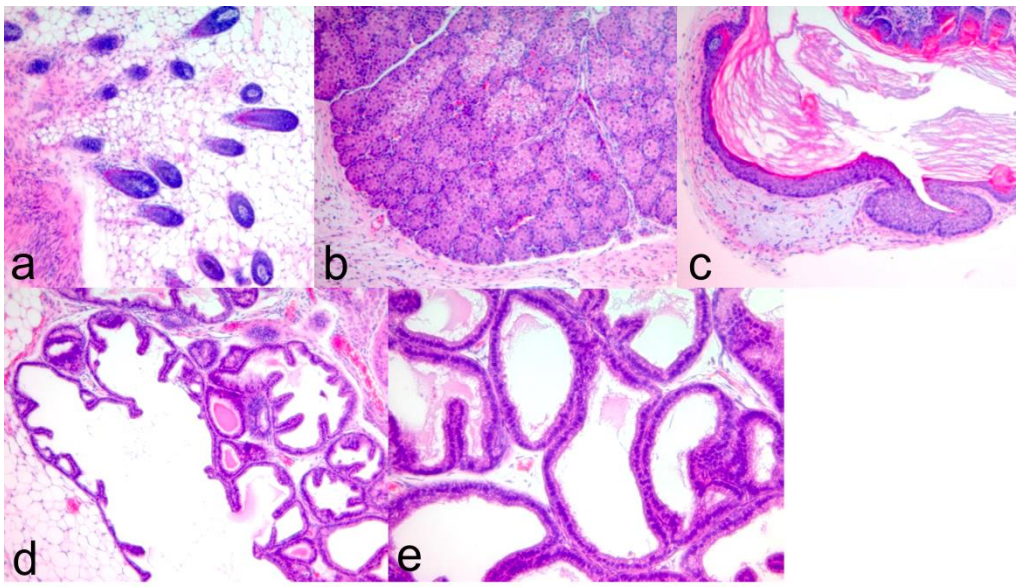

B

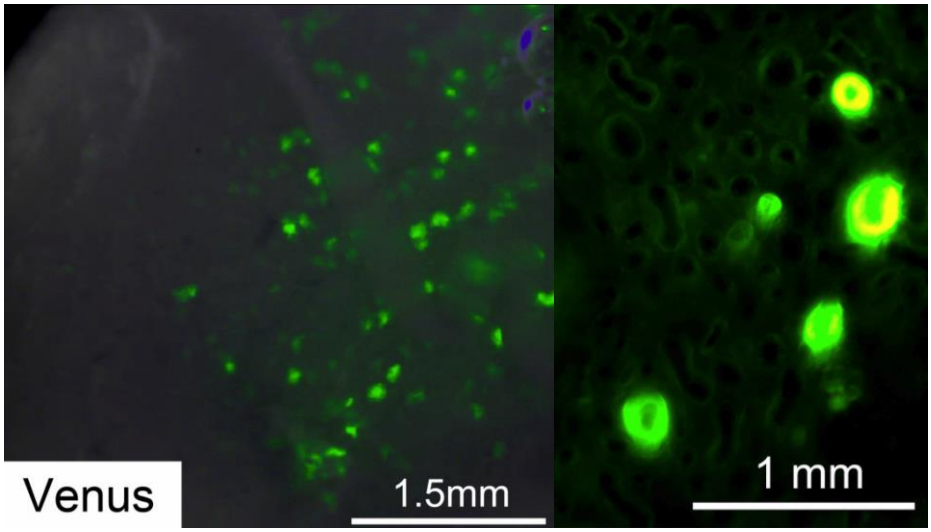

C

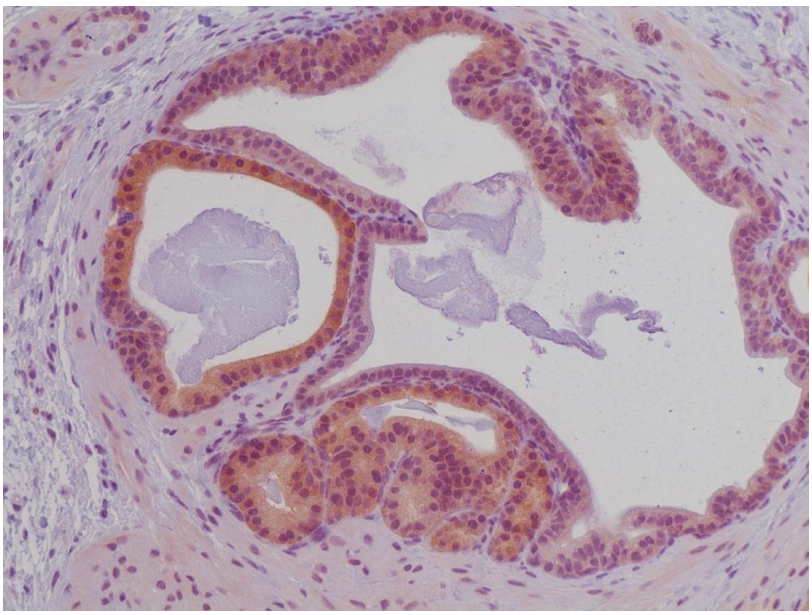

Figure S7, related to Figure 7

Cultured and enriched basal PESCs preserve functional adult stem cell capacity *in vivo*

(A) We transplanted freshly dissected E16 urogenital sinus mesenchyme (UGSM) alone subcutaneously into the flanks of 8 week old male nude mice. After 10 weeks we observed growth of small tumors in the flank of these mice. After harvesting grafts we performed H&E staining and could detect the development of various differentiated tissue structures out of E16 UGSM alone. We though could not detect neuronal tissue (negative Synaptophysin staining, not shown) Thus, E16 UGSM alone has to be considered as oligopotent undifferentiated tissue/cells illustrating the importance to specifically mark co-transplanted cultured PESCs (Venus/GFP in our study) to distinguish them from tissues derived from UGSM alone; (a) Morphology of hair like structures, H&E; (b) Morphology of pancreatic like islets, H&E; (c) Morphology of squamous like epithelia, H&E; (d-e) Morphology of prostate like glands, even remnants of corpora amylacea can be detected (small hyaline masses typically found in lumina of prostate glands), H&E. **(B)** Venus positivity of $CD49f^{+}/TROP2^{high}$ derived prostate acini *in vivo*. Directly visualized s.c. growth of regenerated prostatic acini, derived from $Venus^{+}$ $CD49f^{+}/TROP2^{high}$ cultured and expanded cells as detected by fluorescence stereomicroscope at different magnifications. **(C)** Venus (GFP) staining indicate monoclonal derived prostate acini *in vivo*. Slide demonstrating regenerated prostatic tubules that are Venus/GFP positive, thereby demonstrating their origin from the culture (with 200x magnification). The figure additionally demonstrates uniform expression of cells within a single acinus, whereas the neighbouring acini demonstrate Venus positivity too, but with another intensity, again with comparable staining intensities in neighbouring cells. This indicates that regenerated prostatic tubules derived from monoclonal cell origin (Gaisa et al., 2011).

Table S1, related to Figure 1-3

Media composition and components used in this study.

	Mouse Prostate Media (MPM)	**Human Prostate Media (HPM)**
a	Advanced DMEM/F12 (liquid)	Advanced DMEM/F12 (liquid)
b	L-Glutamine	L-Glutamine
c	EGF	EGF
d	bFGF	bFGF
e	Long R^3 IGF-I	Long R^3 IGF-I
f	Transferrin	Transferrin
g	Insulin	Insulin
h	Glucose	Glucose
i		Sodium selenite
j		Progesterone

Cells were plated together with 10µM Y27632 Rock-Inhibitor (Tocris Bioscience)

a. We used Advanced Dulbeccos's Modified Eagle Medium / Ham's F-12 (DMEM/F12) as starting media. It contains additional ethanolamine, glutathione, ascorbic acid, insulin, transferrin, AlbuMAX®I lipid-rich bovine serum albumin, sodium selenite, ammonium metavanadate, cupric sulfate and manganous chloride, the complete formulation and concentrations can be found at the manufacturers website (Gibco, Invitrogen).

b. L-glutamine 200mM (100x), liquid from Gibco Life Technologies™, used 292 µg ml^{-1}.

c. Recombinant human epidermal growth factor (EGF) from Peprotech (animal-free), used 100ng ml^{-1}.

d. Recombinant human fibroblast growth factor-basic (FGF-2) from Peprotech (animal-free), used 100ng ml^{-1}.

e. LONG® R^3 IGF-I, recombinant analog of human insulin-like growth factor-I from Sigma, used 20ng ml^{-1}.

f. Holo-transferrin, human from Sigma, used 10 µg ml^{-1}.

g. Insulin, human from Sigma, used 20 µg ml^{-1}.

h. D-(+) Glucose solution, 45% in H_2O, from Sigma, used 150 ng ml^{-1}.

i. Sodium selenite, from Sigma, used 14 ng ml^{-1}.

j. Progesterone, from Sigma, used 20 ng ml^{-1}.

Additionally used media components during the development of murine and human culture conditions

Components and used concentration	**Company**
Hydrocortisone, 100nM, 36ng ml^{-1}	Sigma
BSA (1%)	Millipore
Heparine, 80 µg ml^{-1}	Sigma
N2 supplement (100x, liquid), 10µl ml^{-1}	Invitrogen
2-Mercaptoethanol (BME), 50mM (1000x. liquid), 7.8 µg ml^{-1}	Invitrogen
Trace elements A (1000x, liquid), 1µl ml^{-1}	Mediatech/Cellgro
Trace elements B (1000x, liquid), 1µl ml^{-1}	Mediatech/Cellgro
Trace elements C (1000x, liquid), 1µl ml^{-1}	Mediatech/Cellgro
PrEGM™ (Prostate Epithelial Cell Growth Medium) plus BulletKit	Lonza
Fetal bovine serum (FCS), 2-5%	Sigma
Bovine pituitary extract (BPE), 30 µg ml^{-1}	Sigma

Table S2, related to Figure 3

Patients characteristics

(of which human prostatic tissue was obtained during surgery and used in this study)

Patient age	Pathology report	Prostate Size	PSA /serum ng/ml
67	Benign prostatic hyperplasia	23 ml	2.5
69	Benign prostatic hyperplasia	53 ml	3.8
80	Benign prostatic hyperplasia	85 ml	4.8
88	Benign prostatic hyperplasia	40 ml	1.8
82	Benign prostatic hyperplasia	35 ml	1.5
73	Benign prostatic hyperplasia	28 ml	3.2
74	Benign prostatic hyperplasia	30 ml	1.8
59	Benign prostatic hyperplasia	35 ml	2.3

Table S3, related to Figure 6

Pathways upregulated in PESCs as compared to the more differentiated sphere cells, as discovered by GSEA with FDR < 0.001

Table S4, related to Figure 7

Additional prostate regeneration assays. Transplantation results of cultured Lego V2/T2 transduced CD49f^{+}/TROP2^{high} cells together with or without E16 UGSM (Cunha and Lung, 1978; Xin et al., 2003).

Positive graft formation was evaluated after 10-12 weeks in vivo by stereomicroscope (GFP channel) positivity of freshly dissected grafts as well as histological evaluation (anti-GFP/Venus antibody).

Murine CD49f^{+}/TROP2^{high} cells (without UGSM) in s.c. transplantation (male mice)

No. CD49f^{+}/TROP2^{high}	Nude mice	NOD/SCID mice
1x10^{4}	**0/5**	**0/5**
1x10^{5}	**0/5**	**0/5**
0.5x10^{6}	**0/5**	**0/5**
1x10^{6}	**0/5**	**0/5**

Murine CD49f^{+}/TROP2^{high} cells together with E16 UGSM, renal capsule transplantation (male mice)

No. CD49f^{+}/TROP2^{high}	Nude mice	
5x10^{4}	**3/10**	

Murine CD49f^{+}/TROP2^{high} cells, intraprostatic transplantation (without UGSM, male mice)

No. CD49f^{+}/TROP2^{high}	Nude mice	NOD/SCID mice
0.5x10^{6}	**0/10**	**0/8**

Human CD49f^{+}/TROP2^{high} cells together with E16 UGSM, renal capsule transplantation (male mice)

No. CD49f^{+}/TROP2^{high}	Nude mice	NOD/SCID mice
5x10^{4}	**0/10**	**0/10**

Human CD49f^{+}/TROP2^{high} cells, intraprostatic transplantation (without UGSM, male mice)

No. CD49f^{+}/TROP2^{high}	Nude mice	NOD/SCID mice
0.5x10^{6}	**0/5**	**0/5**

Table S5

Antibodies used in this study (FACS/MACS/ immunofluorescence /immunohistochemistry)

FACS	Dilution	Company	Clone/Order#
anti-Human			
CD49f-PE	1:333	eBioscience	GoH3
TROP2-APC	1:100	R&D Systems	FAB650A
CD31-FITC	1:200	BD Pharmingen	M89D3
CD45-FITC	1:250	BD Pharmingen	HI30
CD326 (EPCAM)-PE	1:10	Miltenyi Biotec	HEA-125
anti-Mouse			
TER119-FITC	1:250	eBioscience	TER-119
CD31-FITC	1:250	eBioscience	390
CD45-FITC	1:250	eBioscience	30-F11
CD49f-PE	1:333	eBioscience	GoH3
SCA-1-PE-Cy7	1:500	Biolegend	E13-161.7
TROP2-Biotin	1:100	R&D Systems	BAF1122
SA-APC	1:200	eBioscience	17-4317-82
CD326 (EPCAM)-PE	1:250	eBioscience	G8.8
MACS			
anti-Human			
CD326 (EPCAM) Microbeads	1:5	Miltenyi Biotec	130-061-101
indirect magnetic bead labeling			
Anti-PE microbeads	1:5	Miltenyi Biotec	130-048-801
Immunofluorescence/ Immunohistochemistry			
Cytokeratin 5	1:500	Covance	PRB-160P
Cytokeratin 8	1:500	Covance	MMS-162P
Cytokeratin 5 (IF)	1:500	Abcam	ab128190
Cytokeratin 8 (IF)	1:500	Santa Cruz	sc-101459
p63 (IHC+IF)	1:200	Santa Cruz	4A4 (sc-8431)
Androgen Receptor (AR)	1:200	Santa Cruz	N-20 (sc-816)
NKX 3-1 (mouse)	1:100	Thermo Scientific	MA1-16906
NKX 3-1 (mouse)	1:100	Santa Cruz	M-96 (sc-25406)
Anti-GFP/Venus	1:500	Abcam	ab290
NME1-NME2	1:25	Sigma Aldrich	HPA008467
PAK1	1:250	Santa Cruz	C-19 (sc-881)
PRDX1	1:100	Sigma Aldrich	HPA007730
Lamin B1	1:200	Santa Cruz	sc-6216
TROP2-Biotin	1:10	R&D Systems	BAF1122
AMACR	1:200	Dako	13H4
CD138 (Syndecan-1)	1:100	Sigma Aldrich	HPA006185
CD51/ITGAV	1:100	Sigma Aldrich	HPA004856

CD49b	1:25	Santa Cruz	sc-74466

Supplementary Experimental Procedures

RNA purification and Gene-Expression analyses

Total RNA was isolated from single cells and spheres by directly lysing ~80% confluent cultures using the miRNeasy kit as described (Qiagen, Hilden). RNA was isolated in passage 5 of the culture. Prostaspheres were retrieved out of Matrigel before using Cell Retrieval Solution (BD). Gene expression analysis was performed using the Illumina BeadChip Technology (HumanHT-12 v4 for human cells and Mouse WG-6 v2.0 for murine cells) in the DKFZ genomics core facility unit (GPCF, DKFZ, Heidelberg). For all analyses of differential gene expression and clustering we employed the TM4 Microarray Software Suite (Saeed et al., 2003). Significant Analysis of Microarray (SAM)(Tusher et al., 2001) was used to identify differentially regulated genes between conditions selected at a FDR < 0.05 and with a fold change of > 2. Correlation plots and respective Pearson coefficients (R^2) between samples were generated using 'R' (The R Project for Statistical Computing, http://www.r-project.org/). At least three biological replicates were used for each analysis.

Gene Set Enrichment Analysis

Gene Set Enrichment Analysis (GSEA) (Subramanian et al., 2005) was conducted on median-centred normalized data from murine and human prostate cells independently. Briefly, enrichment of genesets of the curated and motif gene sets database (c2 and c3 in MSigDB) was analysed, thereby comparing spheres versus single cells for both species independently. GSEA was based on ranking genes according to their fold change for the indicated variables. The output of GSEA is an enrichment score (ES), a normalized enrichment score (NES) which accounts for the size of the gene set being tested, a p-value and an estimated False Discovery rate (FDR). We computed p-values using 1,000 permutations for each geneset and adjusted them with the FDR method (Subramanian et al., 2005).

A certain geneset was considered to be significantly enriched in one of the two groups when the FDR was lower than 0.2 for the corresponding geneset. We generated independent lists of genesets significantly enriched in spheres and single cells respectively for both human and murine cells. Next we compared the top-ranking genesets of these lists to identify a predicted functional overlap between murine and human signaling in either single cells or spheres.

High-throughput screening of cell surface proteins by flow cytometry

We prepared single cell suspensions of $150x10^6$ cells from each murine and human culture cells using StemPro-Accutase (GIBCO) corresponding to culture passage 7 and 8. After washing and 40µm filtration cells were stained in 96 wells with 242 anti-human monoclonal antibodies or 176 anti-mouse monoclonal antibodies using BD Lyoplate™ Cell Surface Marker Screening Panels. After washing, cells were resuspended in stain buffer (PBS supplemented with 5mM EDTA) and propidium iodide was added to all wells to exclude dead cells during flow cytometry. Flow cytometry screening (Alexa 647 signals) was performed using a BD FACSArray™ Bioanalyzer system, final analysis was done with FlowJo software, Tree Star, Inc.

Lentiviral NF-kB reporter and functional assays

Adherent human prostate basal PESCs of the $CD49f^+/TROP2^{high}$ phenotype were transfected with a lentiviral reporter construct for the transcription factor NF-kB. The underlying pV2b-NF-kB vector was kindly provided and cloned by C. Eisen. It is based on the known Lego V2-vector of Kristoffer Weber (Weber et al., 2008). In the Lego V2 vector, the SFFV promoter above the fluorescence marker Venus, a variant of GFP, was replaced by a minimal CMV promoter using the restriction sites NheI/BamHI. Above this promoter, the NF-kB responsive element was inserted using the restriction sites NheI and NotI. It consists of eight consecutive consensus binding sites for the transcription factor NF-kB (GGGACTTTCC). Thus, the expression of the marker Venus directly correlated with the activity of NF-kB, as this will only be expressed when nuclear NF-kB is active in the cells. Above the restriction sites EcoRI/BsrGI another fluorescence marker (TagBFP, blue fluorescent protein) was

inserted under the control of the Elongation Factor 1 alpha promoter. This is expressed constitutively and thus serves as control of the transduction efficiency. Transduced cells can therefore be measured in the Pacific Blue Channel of the flow cytometer. Thus, cells that are positive for BFP after transduction and at the same time demonstrate a positivity for Venus (FITC/PB channels) demonstrate an active transcription factor NF-kB activity, evaluable in living cells (Gilmore, 2006). We sowed transduced human PESCs at a ratio of 1:1 at the same time in the HPM-established culture condition and in the sphere conditions. Additionally we tested various media conditions (for 6 hours) on the adherent growing PESCs. We tested the HPM-condition against HPM-basal (HPM medium without growth factors) and additionally compared to PrEGM medium (with all the associated growth factors including dihydrotestosterone). The latter is normally used as a differentiation medium on the spheres/matrigel mix and should clarify as a separate test parameter, whether PrEGM/DHT medium alone can induce an NF-kB activation. In addition, we treated adherent hPESCs with HPM medium that was supplemented with 50 ng/ml or 100 ng/ml TNFα. Ultimately, cells treated with different media conditions as well as sphere cells were examined simultaneously by cytometry. Further functional analyses were done by comparing hPESCs in different sphere conditions. We compared the sphere forming capacity in separate wells: hPESC in standard Matrigel/PrEGM conditions as compared to Matrigel/PrEGM supplemented with either JSH-23 or Etanercept. To block nuclear translocation of the p65 subunit of NF-kB, JSH-23 was used at a concentration of 75 µM (Kesanakurti et al., 2013; Shin et al., 2004). To block soluble TNFα mediated TNFR binding we used Etanercept at a concentration of 5 µg/ml. During the usual sphere forming routine, PREGM+DHT and inhibitors were supplemented fresh every 48h (Lukacs et al., 2010; Xin et al., 2007).

Multiplex fluorescence in situ hybridization (M-FISH)

M-FISH was performed as described by Geigl et al. (Geigl et al., 2006). Briefly, seven pools of flow-sorted human whole chromosome painting probes were amplified and directly labeled using seven different fluorochromes (DEAC, FITC, Cy3, Cy3.5, Cy5, Cy5.5, and Cy7) by degenerative oligonucleotide primed PCR (DOP-PCR). Metaphase chromosomes immobilized on glass slides were denatured in 70% formamide/2xSSC pH 7.0 at 72°C for 2 minutes followed by dehydration in a

degraded ethanol series. Hybridization mixture containing combinatorially labeled painting probes, an excess of unlabeled cot1 DNA, 50% formamide, 2xSSC, and 15% dextran sulfate were denatured for 7 minutes at 75°C, pre-annealed at 37°C for 20 minutes and hybridized at 37°C to the denaturated metaphase preparations. After 48 hours the slides were washed in 2xSSC at room temperature for 3x 5 minutes followed by two washes in 0.2xSSC/0.2% Tween-20 at 56°C for 7 minutes, each. Metaphase spreads were counterstained with 4.6-diamidino-2-phenylindole (DAPI) and covered with antifade solution. Metaphase spreads were captured using a DM RXA epifluorescence microscope (Leica Microsystems, Bensheim, Germany) equipped with a Sensys CCD camera (Photometrics, Tucson, AZ). Camera and microscope were controlled by the Leica Q-FISH software and images were processed on the basis of the Leica MCK software and presented as multicolor karyograms (Leica Microsystems Imaging solutions, Cambridge, United Kingdom)

Principle working steps to culture primary murine and human basal PESCs.

Step	Murine basal prostate progenitor cells	Human basal prostate progenitor cells
1	harvest of the urogenital system (placed in CO_2-independent media with1% BSA)	collect fresh human prostate tissue during surgery (placed in CO_2-independent media with 1% BSA)
2	perform prostate microdissection as previously described (Lukacs et al., 2010)	mince tissue into 1mm fragments, with scalpel
3	mechanical dissociation of tissue using gentle MACS dissociator	mechanical dissociation of tissue using gentle MACS dissociator
4	Collagenase I/ DNase I digest (2 hours)	Collagenase IV/ DNase I digest (4 hours)
5	Stop digest with CO_2-independent media containing 10% FBS while passing the mixture through 18-22g needles	Stop digest with CO_2-independent media containing 10% FBS while passing the mixture through 18-22g needles
6	filtering 70µm	filtering 70µm
7	2min Accutase treatment	2min Accutase treatment
8	label cells with EPCAM primary antibody followed by magnetic bead labeling	label cells with EPCAM primary antibody followed by magnetic bead labeling (direct or indirect)
9	MACS EPCAM enrichment	MACS EPCAM enrichment
10	use hydrophobic culture flask (e.g. Cellstar)	use surface-treated Primaria flask
11	resuspend EPCAM enriched cells in	resuspend EPCAM enriched cells in

	MPM plus 10µM Y27632	HPM plus 10µM Y27632
12	add fresh MPM media every 2 days	add fresh HPM media every 2 days
13	passage cells in 75% confluency use Accutase to detach cells	passage cells in 75% confluency use Accutase to detach cells

Antibody validation on dissected whole prostates – for cultured cell and sphere characterization.

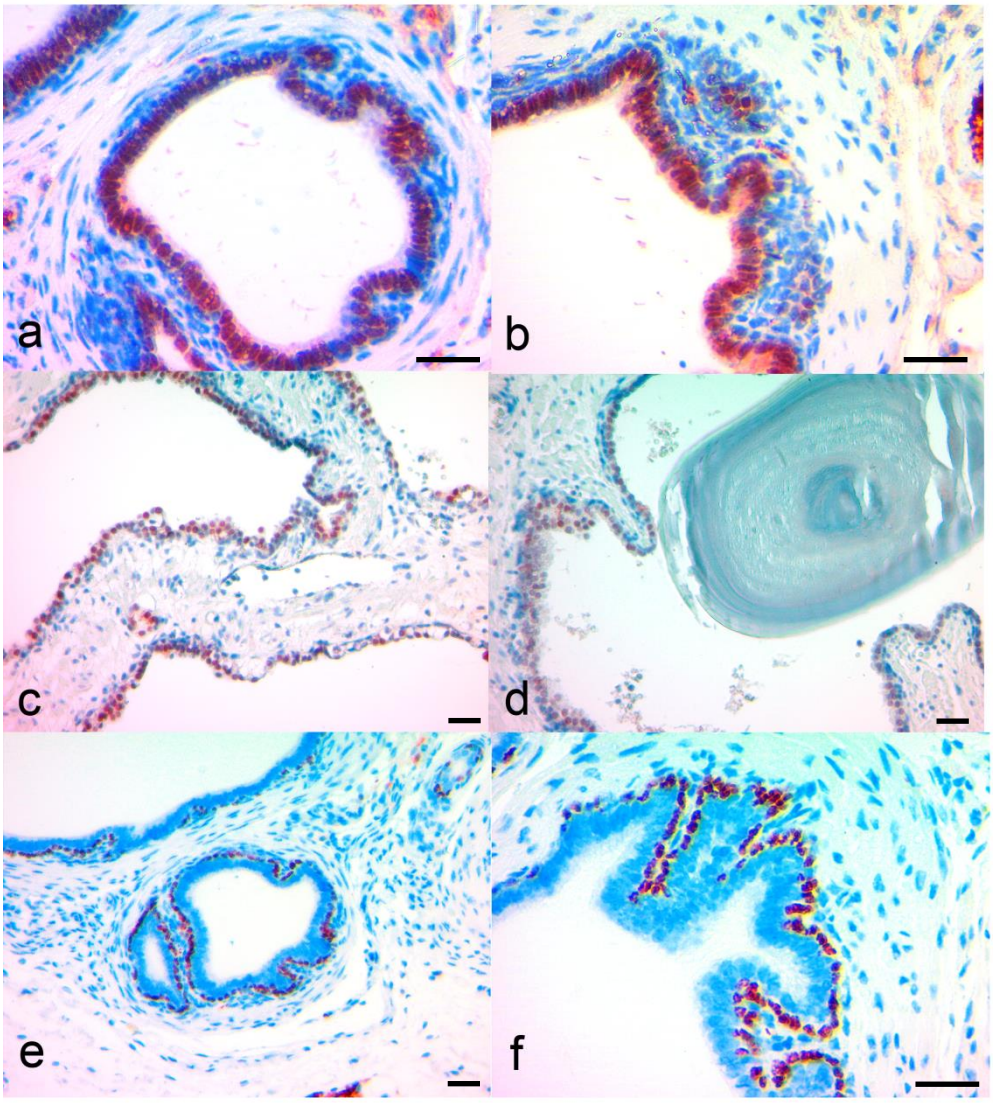

a-b = validation of the Androgen Receptor (AR) antibody on normal murine C57/Bl6 prostate sections (luminal cells)

c-d= validation of the NKX 3-1 antibody on normal murine C57/Bl6 prostate sections (luminal cells)

e-f= validation of the TP63 antibody on normal murine C57/Bl6 prostate sections (basal cells)

References

Cunha, G.R., and Lung, B. (1978). The possible influence of temporal factors in androgenic responsiveness of urogenital tissue recombinants from wild-type and androgen-insensitive (Tfm) mice. J Exp Zool *205*, 181-193.

Geigl, J.B., Uhrig, S., and Speicher, M.R. (2006). Multiplex-fluorescence in situ hybridization for chromosome karyotyping. Nat Protoc *1*, 1172-1184.

Gilmore, T.D. (2006). Introduction to NF-kappaB: players, pathways, perspectives. Oncogene *25*, 6680-6684.

Goldstein, A.S., Huang, J., Guo, C., Garraway, I.P., and Witte, O.N. (2010). Identification of a cell of origin for human prostate cancer. Science *329*, 568-571.

Goldstein, A.S., Lawson, D.A., Cheng, D., Sun, W., Garraway, I.P., and Witte, O.N. (2008). Trop2 identifies a subpopulation of murine and human prostate basal cells with stem cell characteristics. Proc Natl Acad Sci U S A *105*, 20882-20887.

Kesanakurti, D., Chetty, C., Rajasekhar Maddirela, D., Gujrati, M., and Rao, J.S. (2013). Essential role of cooperative NF-kappaB and Stat3 recruitment to ICAM-1 intronic consensus elements in the regulation of radiation-induced invasion and migration in glioma. Oncogene *32*, 5144-5155.

Lukacs, R.U., Goldstein, A.S., Lawson, D.A., Cheng, D., and Witte, O.N. (2010). Isolation, cultivation and characterization of adult murine prostate stem cells. Nat Protoc *5*, 702-713.

Reuter, V.E. (1997). Pathological changes in benign and malignant prostatic tissue following androgen deprivation therapy. Urology *49*, 16-22.

Saeed, A.I., Sharov, V., White, J., Li, J., Liang, W., Bhagabati, N., Braisted, J., Klapa, M., Currier, T., Thiagarajan, M*., et al.* (2003). TM4: a free, open-source system for microarray data management and analysis. Biotechniques *34*, 374-378.

Shin, H.M., Kim, M.H., Kim, B.H., Jung, S.H., Kim, Y.S., Park, H.J., Hong, J.T., Min, K.R., and Kim, Y. (2004). Inhibitory action of novel aromatic diamine compound on lipopolysaccharide-induced nuclear translocation of NF-kappaB without affecting IkappaB degradation. FEBS letters *571*, 50-54.

Subramanian, A., Tamayo, P., Mootha, V.K., Mukherjee, S., Ebert, B.L., Gillette, M.A., Paulovich, A., Pomeroy, S.L., Golub, T.R., Lander, E.S*., et al.* (2005). Gene set enrichment analysis: a knowledge-based approach for interpreting genome-wide expression profiles. Proc Natl Acad Sci U S A *102*, 15545-15550.

Tusher, V.G., Tibshirani, R., and Chu, G. (2001). Significance analysis of microarrays applied to the ionizing radiation response. Proc Natl Acad Sci U S A *98*, 5116-5121.

Weber, K., Bartsch, U., Stocking, C., and Fehse, B. (2008). A multicolor panel of novel lentiviral "gene ontology" (LeGO) vectors for functional gene analysis. Mol Ther *16*, 698-706.

Xin, L., Ide, H., Kim, Y., Dubey, P., and Witte, O.N. (2003). In vivo regeneration of murine prostate from dissociated cell populations of postnatal epithelia and urogenital sinus mesenchyme. Proc Natl Acad Sci U S A *100 Suppl 1*, 11896-11903.

Xin, L., Lukacs, R.U., Lawson, D.A., Cheng, D., and Witte, O.N. (2007). Self-renewal and multilineage differentiation in vitro from murine prostate stem cells. Stem Cells *25*, 2760-2769.